The ROS Wheel: Refining ROS Transcriptional Footprints[1][OPEN]

Patrick Willems, Amna Mhamdi, Simon Stael, Veronique Storme, Pavel Kerchev, Graham Noctor, Kris Gevaert, and Frank Van Breusegem*

Department of Plant Systems Biology, VIB, 9052 Ghent, Belgium (P.W., A.M., S.S., V.S., P.K., F.V.B.); Department of Plant Biotechnology and Bioinformatics, Ghent University, 9052 Ghent, Belgium (P.W., A.M., S.S., V.S., P.K., F.V.B.); Medical Biotechnology Center, VIB, 9000 Ghent, Belgium (P.W., S.S., K.G.); Department of Biochemistry, Ghent University, 9000 Ghent, Belgium (P.W., S.S., K.G.); Institut des Sciences des Plantes de Paris-Saclay, Unité Mixte de Recherche 8618, Centre National de la Recherche Scientifique, Université de Paris-Sud, 91405 Orsay cedex, France (A.M., G.N.); and Unité Mixte de Recherche 9213/Unité Mixte de Recherche 1403, Université Paris-Sud, Centre National de la Recherche Scientifique, Institut National de la Recherche Agronomique, Université d'Evry, Université Paris-Diderot, Sorbonne Paris-Cité, 91405 Orsay, France (A.M., G.N.)

ORCID IDs: 0000-0003-4667-2294 (P.W.); 0000-0001-9959-1362 (A.M.); 0000-0001-8322-0428 (S.S.); 0000-0003-4762-6580 (V.S.); 0000-0003-2737-0493 (P.K.); 0000-0002-4237-0283 (K.G.); 0000-0002-3147-0860 (F.V.B.).

In the last decade, microarray studies have delivered extensive inventories of transcriptome-wide changes in messenger RNA levels provoked by various types of oxidative stress in Arabidopsis (*Arabidopsis thaliana*). Previous cross-study comparisons indicated how different types of reactive oxygen species (ROS) and their subcellular accumulation sites are able to reshape the transcriptome in specific manners. However, these analyses often employed simplistic statistical frameworks that are not compatible with large-scale analyses. Here, we reanalyzed a total of 79 Affymetrix ATH1 microarray studies of redox homeostasis perturbation experiments. To create hierarchy in such a high number of transcriptomic data sets, all transcriptional profiles were clustered on the overlap extent of their differentially expressed transcripts. Subsequently, meta-analysis determined a single magnitude of differential expression across studies and identified common transcriptional footprints per cluster. The resulting transcriptional footprints revealed the regulation of various metabolic pathways and gene families. The *RESPIRATORY BURST OXIDASE HOMOLOG F*-mediated respiratory burst had a major impact and was a converging point among several studies. Conversely, the timing of the oxidative stress response was a determining factor in shaping different transcriptome footprints. Our study emphasizes the need to interpret transcriptomic data sets in a systematic context, where initial, specific stress triggers can converge to common, aspecific transcriptional changes. We believe that these refined transcriptional footprints provide a valuable resource for assessing the involvement of ROS in biological processes in plants.

Excessive levels of reactive oxygen species (ROS) cause cellular stress through damage to all classes of macromolecules and result in cell death. However, ROS also can act as signaling molecules in various biological processes (Van Breusegem et al., 2008; Mittal et al., 2014). In plants, ROS signaling has been documented in environmental stress perception (Suzuki et al., 2012), plant development (Liszkay et al., 2004), cell death (Levine et al., 1994), and the circadian clock (Lai et al., 2012), among others. To allow signaling, a tight regulation of ROS homeostasis is required. Whereas ROS levels can increase through metabolic perturbations leading to incomplete oxygen reduction and through activation of various ROS-producing enzymes, an extensive enzymatic and nonenzymatic antioxidant machinery is in place that tones down excessive ROS levels and thereby cogoverns cellular redox homeostasis (Mittler et al., 2011). Perturbations of ROS homeostasis trigger downstream signaling events via interactions with individual proteins and signaling pathways (Rentel et al., 2004; Tognetti et al., 2012; Herrera-Vásquez et al., 2015). One consequence is the rearrangement of the transcriptome to assist in the protective mechanisms that contribute to the detoxification of ROS and the alleviation or repair of ROS-dependent cellular damage (Mittler et al., 2004). In this manner, transcriptional adjustments are essential to activate long-lasting local and systemic responses that allow improved resilience against subsequent perturbations (Suzuki et al., 2013). Over the past decade, changes in mRNA levels provoked by increased ROS levels have been comprehensively documented in Arabidopsis (*Arabidopsis thaliana*). Transcriptional changes caused by chemical (e.g. inhibitors of mitochondrial and chloroplastic electron transfer chains; Clifton et al., 2005; Jung et al., 2013) and genetic (Vanderauwera et al., 2005; Sewelam et al., 2014) perturbations in ROS- scavenging enzymes, and adverse environmental conditions triggering ROS

production such as high light stress (Oelze et al., 2012; Jung et al., 2013), were monitored in dose- and time-dependent manners, mainly with the Affymetrix GeneChip Arabidopsis ATH1 Genome Array, which monitors levels of more than 20,000 transcripts simultaneously (Redman et al., 2004). In these experiments, the transcriptomes were found to be extensively reshaped. For instance, 2 h of reillumination of the singlet oxygen-generating *fluorescent* (*flu*) mutant caused the increased expression of 1,356 genes (Laloi et al., 2007). A similar number of genes were differentially expressed in catalase (CAT)-deficient plants that accumulate hydrogen peroxide (H_2O_2) under mild photorespiratory conditions (Queval et al., 2012).

Previous comparative studies assessed the relative contribution to changes in gene expression provoked by specific types of ROS, such as H_2O_2 or singlet oxygen ($^1O_2$), and/or by their accumulation in a particular subcellular compartment (Laloi et al., 2007; Sewelam et al., 2014), and demonstrated various ROS transcriptional footprints during developmental processes and abiotic and biotic stress conditions (Lai et al., 2012; Rosenwasser et al., 2013; Mor et al., 2014). To facilitate recognition of ROS transcriptional footprints, a vector-based algorithm, designated ROSMETER was developed (Rosenwasser et al., 2013). In addition, we reanalyzed oxidative stress-related microarray studies from a decade ago (Gadjev et al., 2006). Differentially expressed genes (DEGs) from nine microarray studies were intersected, and sets of general and ROS-specific marker transcripts were proposed (Gadjev et al., 2006). This simplistic, although often used, comparative effort provides a straightforward way to determine a common set of transcriptomic changes and is a good starting point for an initial comparison/assessment of the data sets (Larsson et al., 2006). Our pioneering meta-analysis turned out to be a useful framework for subsequent studies that assessed the involvement of ROS signaling in various biological processes in plants (Jing et al., 2008; Rosenwasser et al., 2011; Peng et al., 2014; Jozefczak et al., 2015).

Despite the usefulness of our previous study, it is clear that it may have been limited by several statistical as well as practical pitfalls. Most importantly, each analysis employed its own methodology and ad hoc criteria to determine DEGs (Larsson et al., 2006). Thereby, the fixed thresholds used to define significant differential expression, such as P value and $\log_2$ fold change (FC), greatly influenced the outcome and thus the interpretation. Moreover, intersection of DEG lists performs no real data integration but rather provides a consistency summary (Tseng et al., 2012). When applied to larger numbers of transcriptomic experiments, it also leads to cumbersome and complex visualization outputs. Another problem is that the identification of robust marker transcripts for specific perturbations among multiple experiments becomes challenging given the inherent biological, experimental, and technical variations (Cahan et al., 2007). Recently, differential gene lists stated to be specific to certain treatments have been advised to be interpreted with caution, especially when DEG lists are intersected to discern specific or common transcriptional changes. It was suggested that the determination of a robust set of ROS marker genes would preferentially take place in consortiums of collaborating laboratories (Vaahtera et al., 2014). The large number of ROS-related microarrays generated by different laboratories encourages identification of such robust signatures by meta-analysis, as demonstrated in this article.

RESULTS

ROS-Related Microarray Data Sets

We compiled the data from 79 independent ATH1 microarray studies (680 CEL files) from diverse experimental setups with disrupted ROS homeostasis (Fig. 1). ROS perturbations were provoked by chemical treatments and genetic modifications, environmental stresses, or combinations thereof. Genetic perturbations contained mutants for antioxidant enzymes (e.g. CAT) and ROS-producing proteins (e.g. respiratory burst oxidase homologs [RBOHs] and glycolate oxidase) but also ROS-related signal transducers and transcriptional regulators. All the microarray studies consisted either of one or multiple (time courses, multiple genotypes, or treatments) transcriptional profiles, resulting in a total of 157 profiles (Supplemental Table S1) that were organized into 12 perturbation categories, each containing between four and 34 profiles (Fig. 1). The largest category comprised ozone (O_3)-, H_2O_2-, and superoxide ($O_2\cdot^-$)-induced signaling, including various mutant backgrounds (seven profiles), chemical treatments with mitochondrial and chloroplastic electron transfer chain inhibitors (eight and 11 profiles, respectively), and direct applications of H_2O_2 (five profiles) or O_3 (three profiles). Besides O_3/H_2O_2/$O_2\cdot^-$, $^1O_2$- (five profiles) and nitric oxide-mediated transcript changes (six profiles)

[1] This work was supported by the Ghent University Special Research Fund (grant no. 01J11311), the Ghent University Multidisciplinary Research Partnership (Ghent BioEconomy grant no. 01MRB510W), the Interuniversity Attraction Poles Programme (grant no. IUAP P7/29), initiated by the Belgian Science Policy Office, Research Foundation- Flanders (grant no. G0D7914N to F.V.B. and J.M. and postdoctoral fellowship to S.S.), the Vlaamse Gemeenschap (grant no. Tournesol T2005.18), and the Agence Nationale de la Recherche (project Cynthiol; grant no. ANR12–BSV6–0011 to G.N.).

* Address correspondence to frank.vanbreusegem@psb.ugent.be.

The author responsible for distribution of materials integral to the findings presented in this article in accordance with the policy described in the Instructions for Authors (www.plantphysiol.org) is: Frank Van Breusegem (frank.vanbreusegem@psb.ugent.be).

P.W. and F.V.B. conceived the project, analyzed the data, and wrote the article with contribution of all coauthors; A.M. and P.K. performed the transcriptomic experiments; V.S. provided statistical assistance; S.S., G.N., and K.G. completed the writing.

[OPEN] Articles can be viewed without a subscription.

www.plantphysiol.org/cgi/doi/10.1104/pp.16.00420

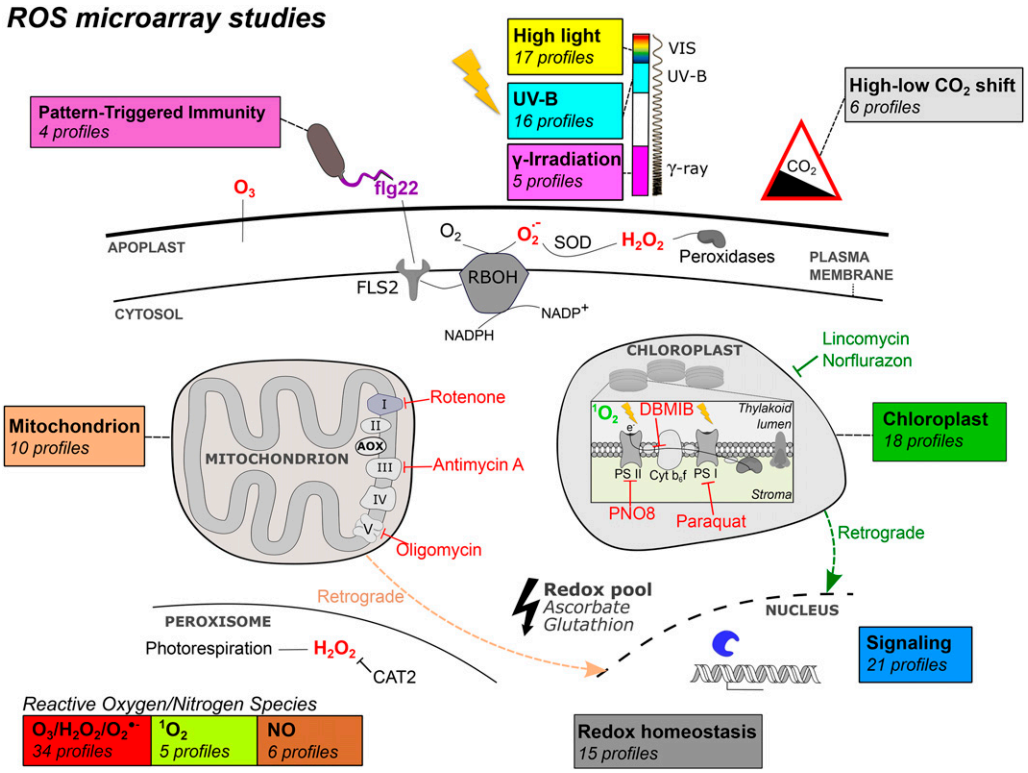

Figure 1. ROS transcriptional profiles and perturbation categories. Transcriptional profiles monitoring ROS homeostasis perturbations were classified under 12 categories (boldface text). For each perturbation category, the number of transcriptional profiles is given. These profiles monitor the transcriptional changes of chemical treatments, environmental stresses, and/or genetic backgrounds. cyt b_6f, Cytochrome b_6f; DMBIB, 2,5-dibromo-6-isopropyl-3-methyl-1,4-benzoquinone; FLS2, FLAGELLIN SENSITIVE2; NO, nitric oxide; PNO8, *N*-octyl-3-nitro-2,4,6-trihydroxybenzamide; SOD, superoxide dismutase; VIS, visible.

were discriminated as separate categories. Besides provoking increased ROS levels, distinction also was made for perturbed redox homeostasis in terms of decreased reductive power due to altered redox pools and reduced scavenging activities (15 profiles), including, among others, ascorbic acid biosynthesis mutants or treatments with antioxidants, such as reduced glutathione. Transcriptional profiles induced by photooxidative stress were included. In total, 17 high-light (HL) profiles were gathered from studies in which plants were shifted from low to high light intensities, and data also were included from analyses of the effect of irradiation with short wavelengths, such as UV-B (290–320 nm; 16 profiles) and γ-rays (less than 10^{-11} nm; five profiles). For the single γ-ray (Culligan et al., 2006) and three UV-B irradiation studies (Ulm et al., 2004; Oravecz et al., 2006; Hahn et al., 2013), a short 15-min irradiation was followed by a recovery in which later time points were sampled. In contrast, two other UV-B studies exposed plants continuously for 1 h, 6 h (Favory et al., 2009), or 24 h (Kusano et al., 2011). To analyze the effects of photorespiratory challenge, studies were included that shifted plants from high to low CO_2 concentrations (six profiles). To represent pathogen challenges, four flagellin22 (flg22)-triggered transcriptional profiles were integrated, because flg22 is known to activate the RBOH-mediated oxidative burst (Li et al., 2014). Our meta-analysis also included 19 transcriptional profiles of reported ROS signaling components, such as transcription factors (TFs), photoreceptors, and retrograde signaling components. As ROS are known signaling compounds in organelle-to-nucleus retrograde communication (Galvez-Valdivieso and Mullineaux, 2010; Ng et al., 2014), our analysis also included separate categories for mitochondrial (10 profiles) and chloroplastic (18 profiles) dysfunctions.

Identifying Similar Transcriptional Changes: the ROS Wheel

All raw microarray data sets (CEL files) were preprocessed simultaneously, and differential expression of 21,430 genes was calculated for all 157 transcriptional profiles (see "Materials and Methods"). DEGs ($P < 0.01$ and $\log_2$ FC > 1) were defined in each profile, resulting in a number of DEGs ranging from 6,430 to only two per profile (specified in Supplemental Table S1). The lowest number of DEGs was found in a 1-h methyl viologen treatment of the experiments performed by the AtGenExpress consortium and is consistent with the relatively low number of DEGs reported previously

for this treatment (Hahn et al., 2013). A large majority of transcriptional profiles (149 out of 157) yielded more than 50 DEGs. Similarity between all transcriptional profiles was scored by their pairwise DEG overlaps according to the Sorensen-Dice similarity coefficient (DSC) with formula $DSC(a,b) = 2\,n_{ab}/(n_a + n_b)$. Thus, as a similarity measure, twice the DEG overlap of studies a and b ($2\,n_{ab}$) was divided by the sum of DEGs present in both studies. It should be noted that the tolerant threshold used to define DEGs ($P < 0.01$) offers more discriminative power between studies. This similarity measure had been employed previously to identify common Arabidopsis transcriptomic responses to different viruses (Postnikova and Nemchinov, 2012). We used the respective dissimilarity (1 – DSC) directly as a distance measure for hierarchical clustering (see "Materials and Methods"). Hence, transcriptomes sharing many DEGs resided in close proximity to each other in the resulting radial clustering tree or ROS wheel (Fig. 2). Clusters below the fixed height cutoff of 0.8 are highlighted (Supplemental Fig. S1) and consist of at least five transcriptional profiles originating from a minimum of two independent studies. These criteria fit our objective to identify common footprints in different microarray studies while at the same time filtering out the clusters from transcriptional profiles originating from the same study.

With these criteria, eight clusters varying in size and perturbation characteristics were found. Cluster I contained four treatments of the chloroplast biogenesis inhibitors lincomycin or norflurazon and four transcriptional profiles of *genome uncoupled* (*gun*) mutants, which are known plastid retrograde signaling components during lincomycin- and norflurazon-provoked chloroplast dysfunction (Koussevitzky et al., 2007). It should be noted that the treatment of wild-type plants was compared against *gun* mutants; thus, the resulting transcriptional profile should be interpreted as a proxy for GUN retrograde signaling. Clusters II and III consisted exclusively of transcription profiles triggered by HL exposures. By comparing the experimental details of the seven HL treatments of cluster II against the five of cluster III, it is clear that factors, such as respective change in light intensity, growth conditions, and developmental age (e.g. leaf versus seedling) do not explain the division between the two clusters. However, a plausible underlying factor might be the duration of light exposure, ranging from 3 to 8 h in cluster II compared with shorter exposures (from 30 min to 2 h) in cluster III. Cluster IV contained a single perturbation category with six $O_3/H_2O_2/O_2\cdot^-$ transcriptional profiles. They originated from two independent studies that administered rotenone and oligomycin to cell cultures, inhibiting the mitochondrial electron transfer chain and ATP synthase, respectively, as well as H_2O_2 treatment of cell cultures (Clifton et al., 2005; Garmier et al., 2008).

The largest cluster was number V, which comprised 20 transcriptional profiles of various compounds that induced ROS directly or indirectly, such as methyl viologen, antimycin A, oligomycin, dibromothymoquinone, *N*-octyl-3-nitro-2,4,6-trihydroxybenzamide, and the flg22 peptide. In addition to these various treatments, the $^1O_2$-generating *flu* mutant, the chloroplastic import mutant *plastid protein import2*, O_3 fumigation, and 3- to 6-h UV-B irradiations were included. Most analyses of the effect of UV-B irradiation were retrieved in cluster VI, which contained eight profiles surveying transcriptional changes after 15 min to 1 h of UV-B, as well as multiple early $^1O_2$-induced transcriptional changes, such as a 30-min dark-to-light shift of the *flu* mutant (Lee et al., 2007), $^1O_2$ accumulation in cell cultures due to HL shift (González-Pérez et al., 2011), or treatment with the photosensitizer Rose Bengal (Gutiérrez et al., 2014). Therefore, we described this cluster as $^1O_2$-UV-B early. A more prolonged reillumination (3 h) of the *flu* mutant was found together with five $O_3/H_2O_2/O_2\cdot^-$ profiles in cluster VII, including a previously unpublished microarray experiment in *rbohF* mutants that we performed to dissect the role of *RBOHF* in secondarily regulating gene expression triggered by H_2O_2 inside the cell (Supplemental Materials and Methods S1). More specifically, the transcriptome of *cat2* mutants grown in long-day air from seeds was compared with that of *cat2 rbohf* double mutants. Hence, the resulting transcriptional changes should be interpreted as the impact of *RBOHF* during oxidative stress.

Lastly, cluster VIII contained five redox mutants, the photosynthesis acclimation double mutant *state transition7 photosystem I subunit e1* (Wassilewskija ecotype; Pesaresi et al., 2009), two mutants in *SUPPRESSOR OF SA INSENSITIVITY OF NPR1-5* (Mandal et al., 2012), a 2-d O_3 treatment, and three UV-B treatments ranging from 12 to 24 h. Given the late timing of these oxidative stress treatments and the presence of constitutively perturbed redox mutants, we termed this cluster ROS acclimation. Both the O_3 study (Booker et al., 2012) and the UV-B studies of the AtGenExpress consortium (Hahn et al., 2013) contained transcriptional profiles of earlier time points that were also present in cluster V, which, as noted above, was the largest ROS cluster. This suggests that cluster V represents transcriptional changes that occur upstream of those present in cluster VIII. Conversely, the $^1O_2$ and UV-B transcriptional profiles of cluster VI contained the 15-min, 30-min, and 1-h time points of the UV-B AtGenExpress study. Thus, the data suggest that the temporal aspect of the oxidative stress responses is an important factor, with transcriptomes from longer oxidative stress exposures (12–48 h) strongly similar to those of constitutively perturbed mutants. In addition to the discussed clusters, interesting relations between other studies also were found. For instance, the *snowy cotyledon3* mutant, which displayed photoinhibition in response to altered CO_2 concentrations (Albrecht et al., 2010), showed similarity to four high-to-low CO_2 shifts and PSI mutations (Pesaresi et al., 2009). As such, our unbiased all-to-all comparison allows the discovery of novel relations between studies and formulation of new hypotheses.

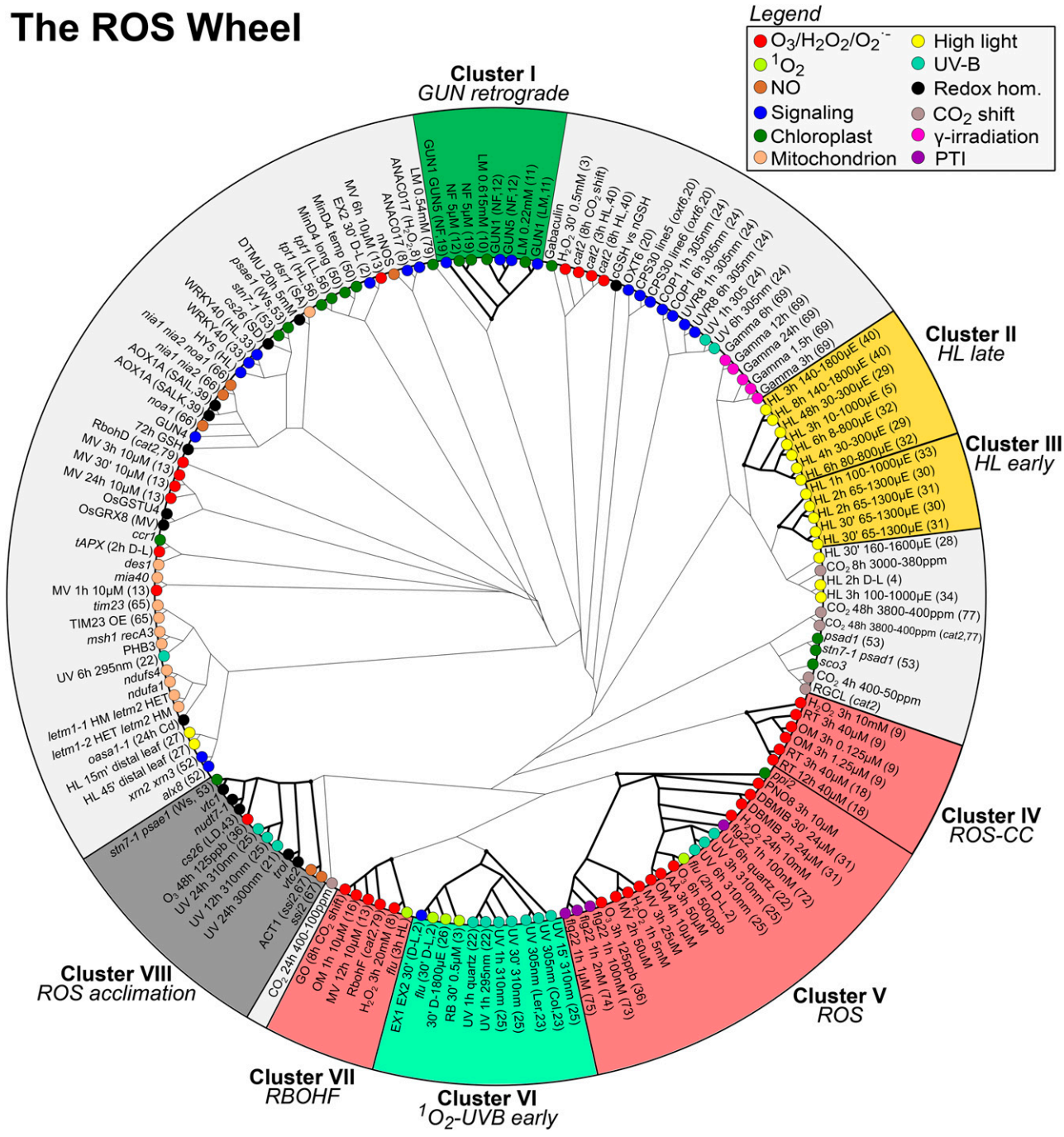

Figure 2. The ROS wheel. All 157 transcriptional profiles were hierarchically clustered according their DEG overlap (see "Materials and Methods"). The hierarchical tree was cut at a fixed height of 0.8 (Supplemental Fig. S1), and clusters that contained at least five profiles, originating from a minimum of two independent studies, are highlighted (clusters I–VIII; thick edges). The numbering of studies is specified in parentheses if a study contained multiple transcriptional profiles. Each profile is accompanied by a circle color coded according to its perturbation category (Supplemental Table S1). CC, Cell cultures; PTI, pattern-triggered immunity.

Random-Effects Models Combining ROS-Induced Transcriptional Changes across Studies

Applied to a large-scale compendium of microarray experiments, our clustering strategy revealed similar transcriptional profiles sharing high numbers of DEGs. As our clustering approach was based on DEG overlaps, genes differentially expressed ($P < 0.01$ and $\log_2$ FC > 1) in all transcriptional profiles of a cluster could be extracted easily. For example, 12 transcripts were differentially expressed in all transcriptional profiles, or

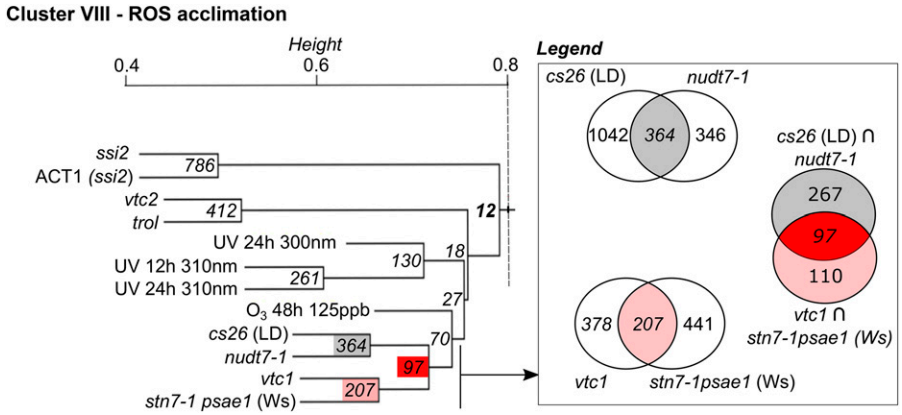

Figure 3. DEG overlaps between transcriptional profiles of ROS acclimation cluster VIII. Cluster VIII was extracted from the hierarchical clustering tree (Supplemental Fig. S1), and the fixed height cutoff is shown (branched line). Node labels specify the DEG overlap between the respective transcriptional profiles or unions thereof (see inset). In total, 12 core DEGs (i.e. differentially expressed in all profiles) were found for cluster VIII (indicated in boldface). Ws, Wassilewskija accession.

core DEGs, constituting acclimation cluster VIII (Fig. 3). For each cluster, the genes differentially expressed in all transcriptional profiles of the respective cluster are presented in Supplemental Table S2. However, such a DEG intersection approach is overly conservative and highly influenced by fixed thresholds.

Striving for a more robust identification of genes that were differentially expressed among the transcriptional profiles of a cluster, we employed an effect-size meta-analysis. We fitted random-effects models (REMs) with the transcript $\log_2$ FC and SE across all transcriptional profiles of a cluster to determine a single expression change (see "Materials and Methods"). Figure 4A shows as an example the REM results for *GLUTAREDOXIN13* (AT1G03850) in cluster VIII. *GLUTAREDOXIN13* transcript levels were not significantly different ($P = 0.052$) in one out of 12 transcriptional profiles of cluster VIII. However, the REM estimated a summarized expression change of 2.27 accompanied by a 95% confidence interval of 1.61 to 2.93. REMs were fitted for all other genes (21,430 in total) in cluster VIII treatments, resulting in the identification of 335 induced and 34 repressed genes (Fig. 4B). We considered a transcript as higher expressed in a cluster when the CILB exceeded a $\log_2$ FC of 0.58 (equal to FC of 1.5) or lower expressed in a cluster when the CIUB was below −0.58. This approach allowed us to recognize relatively small expression changes that were consistent across studies.

Together, the genes showing high ($CI_{LB} > 0.58$) and low ($CI_{UB} < -0.58$) expression in a cluster constitute the transcriptional footprint of the cluster. The transcriptional footprints of each cluster are available in Supplemental Table S3. The largest extent of reprogramming was observed in the early HL cluster III, with a footprint consisting of 803 increased and 861 decreased transcripts (Table I). Some clusters were characterized by a predominant repression or induction of transcripts. For instance, the chloroplast dysfunction cluster I footprint showed a repression of 652 genes, whereas only 33 genes were induced. An opposite scenario is present for the footprints of the *RBOHF* (VII) and early $^1O_2$-UV-B (VI) clusters, in which no decreased transcript levels were observed, but 126 and 264 genes, respectively, were induced. The ROS cluster V footprint was most extensive, with 874 higher and 313 lower expressed genes. We compared the REM-derived transcriptional footprints with the earlier described core DEGs or genes fulfilling the fixed DEG criteria ($P < 0.01$ and $\log_2$ FC > 1) in each profile of a cluster. For each cluster, the core DEGs formed a small fraction of those identified by the REM (Supplemental Fig. S2). For example, only 10 core DEGs occurred in cluster V, whereas the REM identified 1,187 DEGs. Similarly, hundreds of additional DEGs were identified in other clusters. Taken together, the REM provides a statistically robust method to identify differential transcripts that show consistent changes across multiple studies.

Transcriptional Regulation of Pathways and Gene Families under Redox Perturbations

To test whether the obtained transcriptional footprints showed the regulation of biological processes, we performed a gene set enrichment analysis (GSEA) on the induced and repressed genes shaping the REM-derived transcriptional footprints. Enrichment for Gene Ontology (GO) pathways (Kyoto Encyclopedia of Genes and Genomes [KEGG] and PlantCyc) and protein family gene sets was assessed using the PlantGSEA tool (Yi et al., 2013). Several gene sets were overrepresented (false discovery rate [FDR] < 0.05) in the induced or repressed genes of the transcriptional footprints (Fig. 5A; Supplemental Table S4). As anticipated, the GO term response to oxidative stress was enriched in all clusters. In cluster I, chloroplast dysfunction caused an extensive repression of oxidative stress-responsive genes and chloroplast-associated gene sets such as the KEGG pathway photosynthesis (35 genes; FDR = 7.66e-29) and the cellular component GO set chloroplast (519 genes; FDR = 5.49e-304). The GO term respiratory burst was strongly represented (FDR < 1e-25) among the induced genes of the footprints of clusters V to VIII. The oxidative burst is part of the KEGG pathway plant-pathogen interaction, which includes 138 genes (KEGG ath04626). This pathway was enriched among induced genes of the ROS cluster V, early

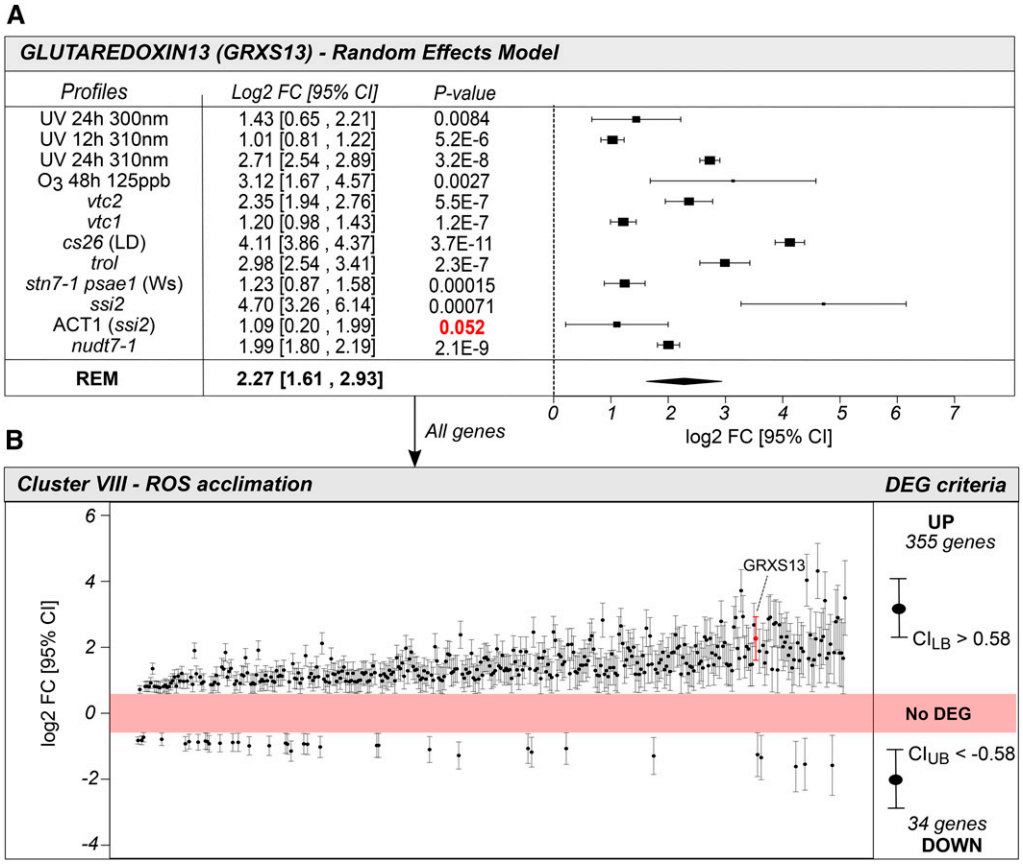

Figure 4. REMs for GLUTAREDOXIN13 and all genes in cluster VIII. A, REM for GLUTAREDOXIN13 (GRXS13; AT1G03850), showing the $\log_2$ FCs with their 95% confidence interval (95% CI) and *P* values ($P > 0.01$ in red) for the 12 transcriptional profiles constituting cluster VIII. The differential expression effect size determined by the REM is indicated at the bottom (boldface text). Ws, Wassilewskija accession. B, Transcriptional footprint of cluster VIII. REMs were fitted for all 21,430 genes (GRXS13 indicated in red), and a gene was considered to be significantly more highly expressed when the lower boundary of the confidence interval (CI_{LB}) was greater than a $\log_2$ FC of 0.58 (FC of 1.5) or less expressed when the upper boundary of the confidence interval (CI_{UB}) was smaller than a $\log_2$ FC of −0.58.

UV-$^1O_2$ signaling cluster VI, and later acclimation cluster VIII footprints. The pathway also included members of overrepresented gene families such as Ca^{2+}-binding proteins with an EF-hand domain and Ca^{2+}-dependent protein kinases, receptor-like kinases (RLKs), and WRKY TFs. Moreover, several APETALA2/ETHYLENE-RESPONSIVE ELEMENT-BINDING PROTEIN and HEAT SHOCK FACTOR families were induced, which is in accordance with their suggested roles as ROS response mediators (Miller and Mittler, 2006, Mor et al., 2014).

Whereas the transcriptional footprints of clusters mostly show enrichment of gene sets with increased or decreased transcript levels, RLKs were enriched among both higher and lower expressed genes of the ROS cluster V footprint. In total, 12 RLKs were repressed in ROS cluster V. Additionally, the early HL cluster III footprint contained several repressed RLKs, 44 in total, of which seven showed similarly decreased expression in ROS cluster V (Supplemental Fig. S3). However, several RLKs had opposite responses between both clusters, with low expression under short HL exposures but more abundant expression in ROS cluster V. Different transcriptional regulation also was observed between early (cluster III) and prolonged (cluster II) light exposures. For instance, more prolonged light exposures in cluster II triggered strong induction of flavonoid biosynthesis genes (FDR = 1.57e-03; Fig. 5B). One example is the TF MYB DOMAIN PROTEIN75, which is the most strongly induced gene in the late HL cluster II footprint ($\log_2$ FC = 4.20, 95% confidence interval 3.58, 4.83) and is a known activator of anthocyanin biosynthesis (Teng et al., 2005). Induction of MYB DOMAIN PROTEIN75 and anthocyanin genes was reported to be impaired in the redox-perturbed vitamin C-deficient mutants *vtc1* and *vtc2* (Page et al., 2012), which are part of cluster VIII. Thus, our GSEA analysis allows the identification of the transcriptional regulation of different biological processes in the footprints.

The Respiratory Burst as a Convergence Point in Transcriptional Imprinting

As indicated by the GSEA analysis, induced genes of clusters IV to VIII footprints were enriched in the

Table I. *DEGs selected from REM results for each cluster*

DEGs were selected based on the CI limits ($CI_{LB} > 0.58$ for increased expression and $CI_{UB} < -0.58$ for decreased expression).

Cluster	Increased Expression ($CI_{LB} > 0.58$)	Decreased Expression ($CI_{UB} < -0.58$)
I, GUN retrograde	33	652
II, HL late	641	581
III, HL early	803	861
IV, ROS cell cultures	202	219
V, ROS	874	313
VI, $^1O_2$-UV-B early	264	0
VII, *RBOHF*	126	0
VIII, ROS acclimation	355	34

respiratory burst GO term. Cluster VII contained the transcriptional phenotype of *RBOHF* under stress. More specifically, the oxidative stress response in the *cat2* mutant was compared with the response in the *cat2 RBOHF* double mutant. Hence, the resulting transcriptional changes should be interpreted as transcriptional changes mediated by *RBOHF* during oxidative stress. As can be observed in Supplemental Table S1, the deficiency of *RBOHF* triggered a more severe transcriptional response (367 DEGs) than *RBOHD* (44 DEGs). *RBOHF* activity is a crucial regulator of pathogen responses and associated metabolic adjustments (Chaouch et al., 2012). Furthermore, *RBOHF* was shown to enhance ROS production and cell death during ozone treatment, unlike *RBOHD* (Xu et al., 2015a). The transcriptional footprint of the *RBOHF*-containing cluster VII was limited to 126 induced genes. As also suggested by the enrichment of the respiratory burst GO term in clusters IV to VIII (Fig. 5A), an *RBOHF*-mediated oxidative burst would be a logical converging point

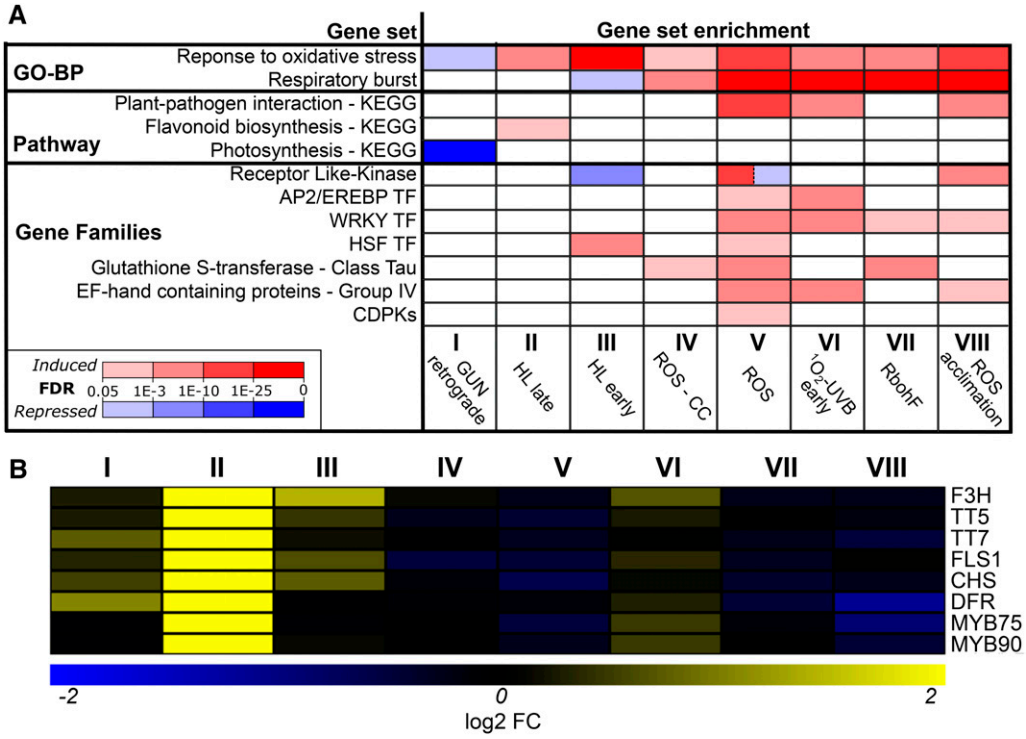

Figure 5. GSEA of transcriptional footprints. A, Up- or down-regulated genes belonging to the transcriptional footprints of clusters I to VIII (columns) were controlled for enrichment in GO biological process (BP), pathway, and protein family gene sets (rows) using the PlantGSEA tool (Yi et al., 2013; see "Materials and Methods"). Enrichment of gene sets (FDR < 0.05) is colored in red (enriched induced genes) or blue (enriched repressed genes) according to their significance (−log FDR). AP2/EREBP, APETALA2 and ETHYLENE-RESPONSIVE ELEMENT BINDING PROTEIN; CDPK, CALCIUM-DEPENDENT KINASE; HSF, HEAT SHOCK FACTOR. B, Heat map displaying the summarized differential expression of flavonoid biosynthesis-associated genes in clusters I to VIII.

resulting in a similar transcriptional footprint across these clusters. To test this hypothesis, we compared the correlation of the summarized $\log_2$ FC of the 126 induced genes of *RBOHF* cluster VII with their summarized expression changes in the footprints of clusters IV to VIII (Supplemental Fig. S4). The correlation and overlap of *RBOHF*-activated genes (cluster VII) was most prominent with cluster V, which consists of 20 diverse ROS profiles. All 126 genes were present in this cluster (Pearson correlation of 42%; Supplemental Fig. S4), indicating that *RBOHF* provokes a transcriptional effect that also is present in a diversity of oxidative stress perturbations. The GSEA analysis of the *RBOHF* cluster VII revealed enrichment of three protein families: glutathione *S*-transferases, WRKY TFs (Fig. 5A), and two mitochondrial alternative oxidases, AOX1d and AOX1a, which are both well-known stress-induced genes (Ng et al., 2014). *RBOHF*-driven changes in expression were imprinted in diverse redox homeostasis-related transcriptomes, which is consistent with the marked effects of the loss of this NADPH oxidase function on cellular redox state, metabolite profiles, and pathogen resistance (Chaouch et al., 2012).

ROS Transcriptional Footprints Are Found in Environmental Stress-Triggered Transcriptional Responses

The transcriptional footprints can be employed directly to hunt for similar transcriptomes in Genevestigator with the signature search functionality (Hruz et al., 2008). The footprint of cluster VIII (355 induced and 34 repressed genes) was used to retrieve perturbations with similar transcriptional changes (Supplemental Fig. S5). Besides the perturbations that are part of the cluster itself (e.g. *vtc2* and *vtc1*), several additional perturbations were retrieved. These included the antioxidant mutant *vitamin E deficient2* (Maeda et al., 2014), Ca^{2+} signaling *calmodulin binding transcription activator* mutants, and the Ca^{2+}/H^{+} exchanger double mutant *cax1 cax3*. In addition, deficiency of pathogen resistance genes, such as *ENHANCED DISEASE RESISTANCE1*, incubation with the salicylic acid analog benzothiadiazole (2 d), inoculations with plant pathogens (3 d), and insect-plant interactions (*Bemisia tabaci*; 7 d) were found. Lastly, inclusion of the *suppressor of npr1-1* mutant, which negatively regulates NPR1-mediated SA signaling in systemic acquired resistance (Li et al., 1999), suggested that this cluster could be considered as a transcriptional footprint associated with systemic acquired resistance and systemic acclimation.

We performed the same analysis for the early $^1O_2$-UV-B cluster VI footprint (264 induced genes) mentioned above. High similarities were found with several cold, drought, osmotic, and salt transcriptional profiles (Supplemental Fig. S6). Early osmotic and salt stress time points from the AtGenExpress consortium were retrieved (Hahn et al., 2013). Both abiotic stresses had been considered to display a common plant core environmental stress response (PCESR; Hahn et al., 2013). Representative PCESR genes were defined as 56 genes that were differentially expressed in UV-B, osmotic, salt, and wounding stress (Hahn et al., 2013). This gene set, from which 54 genes were present on the updated probe set annotation (see "Materials and Methods"), was compared with the footprints of clusters V, VI, and VIII. These clusters showed a strong

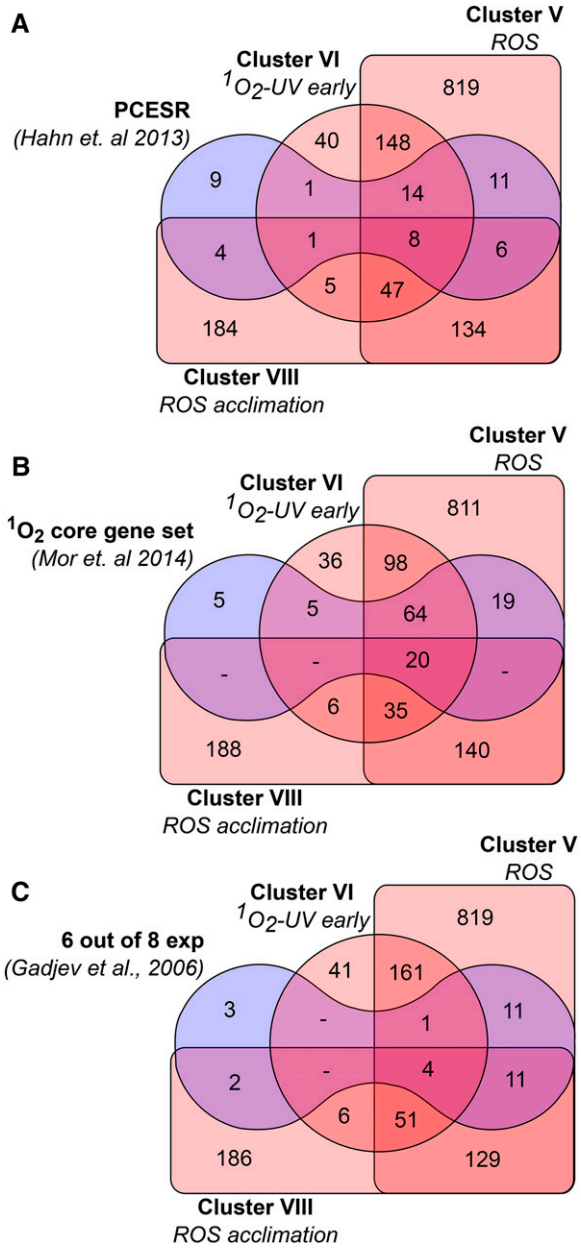

Figure 6. Comparison of transcriptional footprints in clusters V, VI, and VII with the previous meta-analysis. DEG intersection gene lists described by Hahn et al. (2013; A), Mor et al. (2014; B), and Gadjev et al. (2006; C) were compared with transcriptional footprints of clusters V, VI, and VIII. Our probe set annotation caused the loss of three of the PCESR and five of the $^1O_2$ core gene sets.

enrichment (FDR < 1e-25) of the GO term respiratory burst (Fig. 5) and were mentioned before to contain transcriptional profiles spaced in time during the oxidative stress response. The comparison of the PCESR gene set (Hahn et al., 2013) indicated that 45 out of 54 (83%) genes overlapped with genes that are part of clusters V, VI, or VIII footprints (Fig. 6A). The footprint of cluster VI had 24 PCESR genes in common, suggesting early $^1O_2$ signaling as an important factor in the environmental stress response. The presence of $^1O_2$ transcriptome footprints in biotic and abiotic stresses was observed previously (Mor et al., 2014). Mor et al. (2014) determined a $^1O_2$-responsive set of 118 core genes by filtering genes differentially expressed in nine out of 12 microarray experiments after 10 min to 1 h of stress. The footprints of clusters V and VI reported in total 95% of this $^1O_2$ core gene set (Fig. 6B) and, in contrast, the ROS acclimation cluster VIII only a small fraction (20 genes) that also was found in ROS cluster V.

Finally, the meta-analysis conducted by our laboratory a decade ago reported 32 marker transcripts that were differentially expressed in at least six of the eight ROS-related microarrays (Gadjev et al., 2006). The footprints of clusters V, VI, and VIII reported 29 of these 32 genes (91%; Fig. 6C). Thus, our analysis here reveals transcriptional footprints that are consistent with previously conducted stress analyses (Hahn et al., 2013) or ROS-inspired meta-analysis (Gadjev et al., 2006; Mor et al., 2014).

Transcriptional Footprints Are Present in Oxidative Stress RNA Sequencing Studies

RNA sequencing (RNA-Seq) is increasingly used for transcriptomic studies, offering unbiased detection of (low-abundance) transcripts, a broader dynamic range, and improved sensitivity. Unlike the vast amounts of ATH1 microarray data that have documented oxidative stress responses at the transcript level, RNA-Seq studies are still outnumbered. Examples of oxidative stress RNA-Seq studies are a time-course experiment during reillumination of the *flu* mutant (Kim and Apel, 2013) and O_3 treatments in different accessions (Xu et al., 2015a, 2015b). In order to assess transcriptional changes upon photorespiratory stress, we conducted an additional RNA-Seq study in *cat2* mutants after 3 h of stress (Supplemental Materials and Methods S1). This resulted in an extensive transcriptomic reprogramming, with 3,571 significantly induced genes ($\log_2$ FC > 1 and FDR < 0.01) and 2,555 repressed genes ($\log_2$ FC < −1 and FDR < 0.01; Supplemental Table S5). Such high numbers of DEGs also were retrieved after 2 h of *flu* reillumination (3,187 genes; Kim and Apel 2013) or 2 h of O_3 treatment in the wild-type background (5,168 genes; Xu et al., 2015a).

We compared the 404 transcripts induced in the *flu* mutant after 15 min of reillumination (Chen et al., 2015) and the 3,571 induced transcripts in *cat2* after 3 h of photorespiratory stress with the transcriptional footprints of all clusters. It is important to note that genes not present on the microarray platform were filtered from the RNA-Seq study that omitted 631 (*cat2*) and 70 (*flu*) significantly induced genes. The transcriptional footprints showed high consistency with the induced genes of both RNA-Seq studies (Fig. 7). For instance, the induced genes in the *cat2* RNA-Seq study overlapped markedly with clusters IV to VIII. All genes of the *RBOHF* cluster VII footprint were retrieved, whereas approximately 85% to 95% of the footprints of clusters IV, V, VI, and VIII were induced in the RNA-Seq study. Smaller overlaps were observed for short (cluster III; 55%) and prolonged (cluster II; 19%) light exposure signatures. However, *cat2* plants were shifted to excess light for 3 h, which might explain a certain similarity to both HL clusters. Conversely, the *flu* RNA-Seq study shared only one gene with prolonged HL exposures (cluster II). Whereas the ROS acclimation cluster VIII shared 26 induced genes (7.3%) with the 15-min *flu* study, the early $^1O_2$-UV-B cluster VI shared 105 DEGs, or 40% of the signature (Fig. 7). However, nearly all of these overlapping genes also were present in the 3-h *cat2* study (102 DEGs), suggesting that elevated transcript levels of these genes are not restricted to early $^1O_2$ signaling. Besides the *cat2* and *flu* experiments, O_3 RNA-Seq studies (Xu et al., 2015a, 2015b) also were highly consistent with our transcriptional footprints. For instance, induced genes of the ROS cluster V footprint

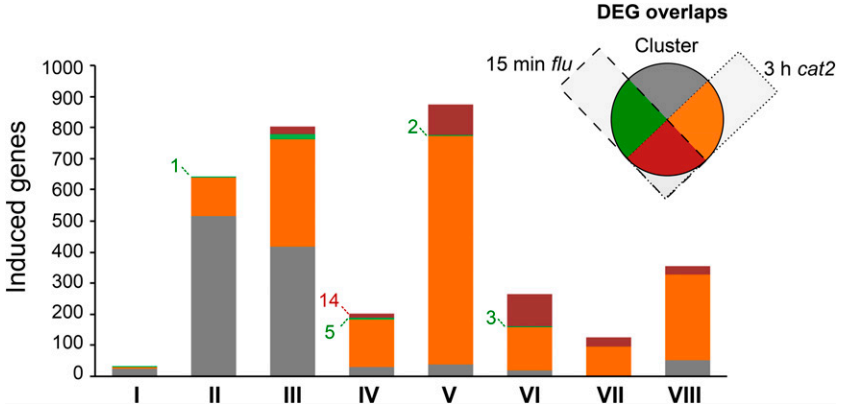

Figure 7. Overlap of induced gene transcriptional footprints and RNA-Seq studies. All induced genes (CI_{LB} > 0.58) of clusters I to VIII intersected with those from the 15-min *flu* and 3-h *cat2* RNA-Seq studies (FDR < 0.01, $\log_2$ FC > 1). The transcriptional footprints (*x* axis) are colored according to their overlap with both RNA-Seq studies, with induced genes either not overlapping (gray) or induced in the 15-min *flu* (green), 3-h *cat2* (orange), or both RNA-Seq (dark red) studies.

were more than 90% present in O_3 treatments performed in multiple Arabidopsis accessions (Xu et al., 2015a, 2015b), as shown in Supplemental Figure S7. Hence, our footprints also can be implemented on data obtained from RNA-Seq and support the biological relevance of our meta-analysis results.

DISCUSSION

Through a large-scale comparison of 79 ROS-related microarray studies (Fig. 1; Supplemental Table S1), we identified similar transcriptional profiles based on their extent of DEG overlap. Eight clusters of similar transcriptional profiles were obtained by hierarchical clustering and visualized in a circular clustering tree (ROS wheel; Fig. 2) that served as a starting point for a meta-analysis on the identified clusters. To determine a representative footprint, robust effect-size statistics were used to determine a single magnitude of differential expression for each cluster (Fig. 4). For each cluster, significantly induced or repressed genes shaped a representative ROS transcriptional footprint. The main insights from our study are that ROS footprints do not seem to correlate directly with subcellular production site or chemical type but that the timing of oxidative stress is a more determining factor. Our meta-analysis emphasizes the interpretation of ROS- or stress-related transcriptional changes in a mechanistic framework with the oxidative burst as a converging point after stress perception, eventually giving rise to systemic ROS-mediated acclimation.

Timing of Oxidative Stress Responses as the Determining Factor in Shaping the Transcriptome

Previously reported meta-analyses, including ours, of oxidative stress-related transcriptional responses mainly described transcriptional changes specific to subcellular production site or chemical type, which are governed by a complex, yet to be elucidated mechanism (Gadjev et al., 2006; Shapiguzov et al., 2012; Vaahtera et al., 2014). Our meta-analysis shows that ROS transcriptional footprints are determined primarily by temporal aspects. For instance, the ROS wheel indicates a footprint between several mutants affected in reducing power in the ROS acclimation cluster VIII (Fig. 3). Such redox homeostasis mutants are constitutively perturbed, unlike the induced ROS accumulation triggered in other transcriptional profiles. Using the REM-derived transcriptional footprint of cluster VIII in the Genevestigator signature search tool revealed several microarray experiments with similar transcriptional footprints relating to salicylic acid-mediated systemic signaling during defense responses. During defense responses, salicylic acid signaling is preceded by oxidative bursts in different cellular compartments (Herrera-Vásquez et al., 2015). The GO term respiratory burst was strongly enriched (FDR $<$ 1e-25) in the footprints of clusters V to VIII. Furthermore, cluster VII contained an *RBOHF* transcriptional profile. The transcriptional footprint of this *RBOHF* cluster consisted of 126 induced genes, and all of them also were induced in the largest ROS cluster V. This cluster was composed of 20 transcriptional profiles, including direct applications of O_3, H_2O_2, flg22, or of electron transfer chain-blocking chemicals, $^1O_2$ provocations, a chloroplast import mutant, and 3 to 6 h of UV-B exposure. Interestingly, the 3- to 6-h O_3 and UV-B perturbations belonged to a study in which later time points were part of the ROS acclimation cluster VII. Conversely, early $^1O_2$-UV-B cluster VI consisted solely of early (15 min to 1 h) UV-B studies and different $^1O_2$ signaling studies using Rose Bengal (Gutiérrez et al., 2014), HL treatments (González-Pérez et al., 2011), or *flu* reillumination (Laloi et al., 2007). The 30-min *flu* reillumination was suggested previously by the ROSMETER as a unique $^1O_2$ response (Rosenwasser et al., 2013), unlike the probably less specific ROS responses at later time points. The early $^1O_2$-UV-B footprint of cluster VI in our meta-analysis was highly consistent with a previously defined DEG set of a core plant stress response (Fig. 6B; Hahn et al., 2013) and supports the $^1O_2$-responsive gene set found in early stress responses (Fig. 6C; Mor et al., 2014). Footprints associated with specific (subcellular) types of ROS probably exist, although they do not seem to be major discernible factors among diverse studies, except the early $^1O_2$ footprint of cluster VI. We believe that the notion of specificity might have been used too easily, as stated before by Vaahtera et al. (2014). Incorrect interpretations can arise from the simplistic approach of previous meta-analyses but also due to the logical fact that specific, initial triggers can result later in converging (aspecific) transcriptional changes.

Determining Robust ROS Transcriptional Footprints

Recently, it had been proposed to use transcriptional marker signatures consisting of several genes instead of single marker genes to study ROS-specific transcriptional regulation (Vaahtera et al., 2014). The development of such representative ROS marker signatures would preferentially take place in a consortium of collaborating laboratories (Vaahtera et al., 2014). Here, we determined robust ROS transcriptional footprints by reanalyzing the results of 79 studies derived from 45 different laboratories. Inherently, this kind of analysis brings various interexperimental variability, due to factors such as laboratory-specific effects, development effects, and within-study variation. Previous microarray meta-analyses indicated that a robust statistical analysis is impossible due to such inherent heterogeneity of various experimental setups (Gadjev et al., 2006; Schwarzländer et al., 2012). Nevertheless, size-effect models are capable of combining independent microarray data (Choi et al., 2003; Stevens and Doerge, 2005; Larsson et al., 2006). An effect-size meta-analysis was implemented recently for Arabidopsis microarray

data (Rest et al., 2016), demonstrating to be a powerful approach to establish robust DEG sets. Here, we fitted REMs to determine a single differential expression effect across transcriptional profiles constituting a cluster (Fig. 4). The REM weighs transcriptional changes by the sum of true variation among studies and sampling within studies, providing effect sizes based on differential expression. Whereas multiple methods exist to correct for variation (Cheng et al., 2009; Chen et al., 2011), such a procedure was not used here to maintain expression changes related to the diverse experimental setups included in our meta-analysis. REMs were fitted for the eight clusters identified in the ROS wheel (Fig. 2). Significantly induced or repressed genes were identified per cluster, together constituting a representative transcriptional footprint (Table I). Importantly, the REM facilitates the detection of lowly expressed genes, but consistently DEGs, which are missed in single microarray studies and might elucidate new functions for these genes (Rest et al., 2016).

In conclusion, using a meta-analysis of 79 ROS microarray data sets, we were able to identify robust ROS transcriptional footprints that can be a valuable resource for the plant community in future ROS-related research. Such signatures will help both in understanding the mechanisms underlying oxidative stress responses and in evaluating the roles of ROS in a given biological process in plants.

MATERIALS AND METHODS

Microarray Data

In total, 680 CEL files of 79 independent studies were collected from the public repositories Gene Expression Omnibus (GEO; http://www.ncbi.nlm.nih.gov/geo/) and ArrayExpress (http://www.ebi.ac.uk/arrayexpress/), requested from authors, or conducted in-house. The included microarray data were controlled for quality, and four unpublished microarray studies were included (Supplemental Materials and Methods S1).

Microarray Data Processing and Differential Statistics

All raw intensity files were normalized by robust multiarray averaging (Irizarry et al., 2003) using the affy package (version 1.40.0) of R/Bioconductor (Gautier et al., 2004). Probe sets were up to date using The Arabidopsis Information Resource 10 CDF annotation retrieved from BrainArray (The Arabidopsis Information Resource G version 18.0.0 [http://www.brainarray.mbni.med.umich.edu/]; Dai et al., 2005). Differential gene expression was analyzed by the limma package (version 3.18.13) using empirical Bayes-moderated t statistics (Smyth, 2005). Perturbations were contrasted discriminated versus the control condition (ROS/control). In the case of genetic perturbations, wild-type or gain-of-function plants were distinguished against loss-of-function or control lines.

Similarity Transcriptional Profiles and Hierarchical Clustering

DEGs were selected for each transcriptomic response, using $P \leq 0.01$ as a significance threshold and a $\log_2$ FC greater than 1 or less than -1. This relatively tolerant threshold was chosen to select DEGs less restrictively, which would favor discrimination between similar profiles in our clustering analysis. Pairwise similarity between each DEG list was assessed using the DSC:

$$DSC(a,b) = \frac{2n_{a,b}}{n_a + n_b}$$

where n_a and n_b represents the DEGs of two independent studies, treating genes with low or high expression as separate entities. Hence, a DSC from two different experiments will range from 0 to 1, with 1 indicating an identical DEG set. Subsequently, the Dice dissimilarity (1 − DSC) matrix was used as a distance measure for hierarchical clustering (average linkage) in R. Clusters were assigned using a fixed-height threshold (Supplemental Fig. S1). To generate the ROS wheel, the corresponding Newick tree was created using the write.tree function of the ape package (version 3.2; Paradis et al., 2004) in R. The Newick tree was imported and transformed to a radial layout in Dendroscope3 (Huson and Scornavacca, 2012).

REM

Differential expression was combined across studies by fitting a REM. Studies were weighted by the sum of true variation among studies and sampling within studies, providing effect sizes based on differential expression. REMs were fitted for each probe set individually (21,430 in total) using the $\log_2$ FCs and corresponding SE values of all the individual transcriptional profiles constituting a transcriptional cluster. The model for the estimated $\log_2$ FC in study i, denoted as y_i, can be written as:

$$y_i = \theta_i + e_i$$

where θ_i is the true effect of study i and $e_i \sim N\ (0, v_i)$, with v_i the known sampling variance of study i. Variability introduced by differences in the methods of the various studies is accommodated by treating this variability as a random effect:

$$\theta_i = \mu + u_i$$

where μ is the average true effect and $u_i \sim N\ (0, \tau^2)$, with τ^2 the amount of heterogeneity among the true effects.

The metafor package in R (version 1.3-2; Viechtbauer 2010) was used to fit REMs for each gene separately using restricted maximum likelihood to estimate the true average effect and the amount of heterogeneity, τ^2.

GSEA

Functional class enrichment was analyzed with the Plant Gene Set Enrichment Analysis Toolkit (http://structuralbiology.cau.edu.cn/PlantGSEA/; Yi et al., 2013). Gene families were enriched for PlantCyc, KEGG, and GO biological processes and cellular component gene sets using the background for Arabidopsis (*Arabidopsis thaliana*) and running on default parameters.

Accession Numbers

The RNA-Seq data discussed in this article have been deposited in the GEO repository (http://www.ncbi.nlm.nih.gov/geo/) and are accessible through the GEO accession GSE77171. Unpublished microarray studies for 24-h 10 mM H_2O_2 and 400- to 100-ppm CO_2 shift are available under the GEO accessions GSE80200 and GSE80158, respectively. The 24-h restricted gas continuous light in *cat2* mutants and mild photorespiratory stress in *cat2 rbohf* and *cat2 rbohd* double mutants are available under the GEO accessions GSE66365 and GSE81516, respectively.

Supplemental Data

The following supplemental materials are available.

Supplemental Figure S1. Hierarchical clustering tree of transcriptional profiles and cluster identification.

Supplemental Figure S2. Performance REM and traditional DEG list intersection approach.

Supplemental Figure S3. Transcriptional regulation of RLKs.

Supplemental Figure S4. Correlation and overlap of induced DEGs of *RBOHF* cluster VII with ROS cluster V.

Supplemental Figure S5. Use of the cluster VIII footprint in the Genevestigator signature search tool (Hruz et al., 2008).

Supplemental Figure S6. Use of the cluster VI footprint in the Genevestigator signature search tool (Hruz et al., 2008).

Supplemental Figure S7. Overlap ROS cluster V footprint with RNA-Seq results of O_3 treatments.

Supplemental Table S1. Experimental details, perturbation category, and number of DEGs ($P < 0.01$ and $\log_2$ FC > 1) of the transcriptional profiles.

Supplemental Table S2. Core gene sets of clusters I to VIII.

Supplemental Table S3. Cluster I to VIII REM result for all 21,430 genes.

Supplemental Table S4. GESA for lower and higher expressed genes of clusters I to VIII.

Supplemental Table S5. RNA-Seq results after a 3-h photorespiratory stress in *cat2* mutants.

Supplemental Materials and Methods S1. Description of microarray quality control and experimental details from unpublished microarray experiments and RNA-Seq studies.

ACKNOWLEDGMENTS

We thank Olivier Van Aken and Alessandro Alboresi for providing microarray data available to us and Yvan Saeys for helpful discussions during the course of this research.

Received March 20, 2016; accepted May 30, 2016; published May 31, 2016.

LITERATURE CITED

Albrecht V, Simková K, Carrie C, Delannoy E, Giraud E, Whelan J, Small ID, Apel K, Badger MR, Pogson BJ (2010) The cytoskeleton and the peroxisomal-targeted snowy cotyledon3 protein are required for chloroplast development in *Arabidopsis*. Plant Cell **22:** 3423–3438

Booker F, Burkey K, Morgan P, Fiscus E, Jones A (2012) Minimal influence of G-protein null mutations on ozone-induced changes in gene expression, foliar injury, gas exchange and peroxidase activity in *Arabidopsis thaliana* L. Plant Cell Environ **35:** 668–681

Cahan P, Rovegno F, Mooney D, Newman JC, St Laurent G III, McCaffrey TA (2007) Meta-analysis of microarray results: challenges, opportunities, and recommendations for standardization. Gene **401:** 12–18

Chaouch S, Queval G, Noctor G (2012) At*RbohF* is a crucial modulator of defence-associated metabolism and a key actor in the interplay between intracellular oxidative stress and pathogenesis responses in Arabidopsis. Plant J **69:** 613–627

Chen C, Grennan K, Badner J, Zhang D, Gershon E, Jin L, Liu C (2011) Removing batch effects in analysis of expression microarray data: an evaluation of six batch adjustment methods. PLoS ONE **6:** e17238

Chen S, Kim C, Lee JM, Lee HA, Fei Z, Wang L, Apel K (2015) Blocking the QB-binding site of photosystem II by tenuazonic acid, a non-host-specific toxin of *Alternaria alternata*, activates singlet oxygen-mediated and EXECUTER-dependent signalling in *Arabidopsis*. Plant Cell Environ **38:** 1069–1080

Cheng C, Shen K, Song C, Luo J, Tseng GC (2009) Ratio adjustment and calibration scheme for gene-wise normalization to enhance microarray inter-study prediction. Bioinformatics **25:** 1655–1661

Choi JK, Yu U, Kim S, Yoo OJ (2003) Combining multiple microarray studies and modeling interstudy variation. Bioinformatics (Suppl 1) **19:** i84–i90

Clifton R, Lister R, Parker KL, Sappl PG, Elhafez D, Millar AH, Day DA, Whelan J (2005) Stress-induced co-expression of alternative respiratory chain components in *Arabidopsis thaliana*. Plant Mol Biol **58:** 193–212

Culligan KM, Robertson CE, Foreman J, Doerner P, Britt AB (2006) ATR and ATM play both distinct and additive roles in response to ionizing radiation. Plant J **48:** 947–961

Dai M, Wang P, Boyd AD, Kostov G, Athey B, Jones EG, Bunney WE, Myers RM, Speed TP, Akil H, et al (2005) Evolving gene/transcript definitions significantly alter the interpretation of GeneChip data. Nucleic Acids Res **33:** e175

Favory JJ, Stec A, Gruber H, Rizzini L, Oravecz A, Funk M, Albert A, Cloix C, Jenkins GI, Oakeley EJ, Seidlitz HK, Nagy F, Ulm R (2009) Interaction of COP1 and UVR8 regulates UV-B-induced photomorphogenesis and stress acclimation in *Arabidopsis*. EMBO J **28:** 591–601

Gadjev I, Vanderauwera S, Gechev TS, Laloi C, Minkov IN, Shulaev V, Apel K, Inzé D, Mittler R, Van Breusegem F (2006) Transcriptomic footprints disclose specificity of reactive oxygen species signaling in Arabidopsis. Plant Physiol **141:** 436–445

Galvez-Valdivieso G, Mullineaux PM (2010) The role of reactive oxygen species in signalling from chloroplasts to the nucleus. Physiol Plant **138:** 430–439

Garmier M, Carroll AJ, Delannoy E, Vallet C, Day DA, Small ID, Millar AH (2008) Complex I dysfunction redirects cellular and mitochondrial metabolism in Arabidopsis. Plant Physiol **148:** 1324–1341

Gautier L, Cope L, Bolstad BM, Irizarry RA (2004) affy: analysis of Affymetrix GeneChip data at the probe level. Bioinformatics **20:** 307–315

González-Pérez S, Gutiérrez J, García-García F, Osuna D, Dopazo J, Lorenzo Ó, Revuelta JL, Arellano JB (2011) Early transcriptional defense responses in Arabidopsis cell suspension culture under high-light conditions. Plant Physiol **156:** 1439–1456

Gutiérrez J, González-Pérez S, García-García F, Daly CT, Lorenzo O, Revuelta JL, McCabe PF, Arellano JB (2014) Programmed cell death activated by Rose Bengal in *Arabidopsis thaliana* cell suspension cultures requires functional chloroplasts. J Exp Bot **65:** 3081–3095

Hahn A, Kilian J, Mohrholz A, Ladwig F, Peschke F, Dautel R, Harter K, Berendzen KW, Wanke D (2013) Plant core environmental stress response genes are systemically coordinated during abiotic stresses. Int J Mol Sci **14:** 7617–7641

Herrera-Vásquez A, Salinas P, Holuigue L (2015) Salicylic acid and reactive oxygen species interplay in the transcriptional control of defense genes expression. Front Plant Sci **6:** 171

Hruz T, Laule O, Szabo G, Wessendorp F, Bleuler S, Oertle L, Widmayer P, Gruissem W, Zimmermann P (2008) Genevestigator v3: a reference expression database for the meta-analysis of transcriptomes. Adv Bioinformatics **2008:** 420747

Huson DH, Scornavacca C (2012) Dendroscope 3: an interactive tool for rooted phylogenetic trees and networks. Syst Biol **61:** 1061–1067

Irizarry RA, Hobbs B, Collin F, Beazer-Barclay YD, Antonellis KJ, Scherf U, Speed TP (2003) Exploration, normalization, and summaries of high density oligonucleotide array probe level data. Biostatistics **4:** 249–264

Jing HC, Hebeler R, Oeljeklaus S, Sitek B, Stühler K, Meyer HE, Sturre MJG, Hille J, Warscheid B, Dijkwel PP (2008) Early leaf senescence is associated with an altered cellular redox balance in *Arabidopsis cpr5/old1* mutants. Plant Biol (Stuttg) (Suppl 1) **10:** 85–98

Jozefczak M, Bohler S, Schat H, Horemans N, Guisez Y, Remans T, Vangronsveld J, Cuypers A (2015) Both the concentration and redox state of glutathione and ascorbate influence the sensitivity of Arabidopsis to cadmium. Ann Bot (Lond) **116:** 601–612

Jung HS, Crisp PA, Estavillo GM, Cole B, Hong F, Mockler TC, Pogson BJ, Chory J (2013) Subset of heat-shock transcription factors required for the early response of *Arabidopsis* to excess light. Proc Natl Acad Sci USA **110:** 14474–14479

Kim C, Apel K (2013) Singlet oxygen-mediated signaling in plants: moving from flu to wild type reveals an increasing complexity. Photosynth Res **116:** 455–464

Koussevitzky S, Nott A, Mockler TC, Hong F, Sachetto-Martins G, Surpin M, Lim J, Mittler R, Chory J (2007) Signals from chloroplasts converge to regulate nuclear gene expression. Science **316:** 715–719

Kusano M, Tohge T, Fukushima A, Kobayashi M, Hayashi N, Otsuki H, Kondou Y, Goto H, Kawashima M, Matsuda F, Niida R, Matsui M, Saito K, Fernie AR (2011) Metabolomics reveals comprehensive reprogramming involving two independent metabolic responses of Arabidopsis to UV-B light. Plant J **67:** 354–369

Lai AG, Doherty CJ, Mueller-Roeber B, Kay SA, Schippers JH, Dijkwel PP (2012) CIRCADIAN CLOCK-ASSOCIATED 1 regulates ROS homeostasis and oxidative stress responses. Proc Natl Acad Sci USA **109:** 17129–17134

Laloi C, Stachowiak M, Pers-Kamczyc E, Warzych E, Murgia I, Apel K (2007) Cross-talk between singlet oxygen- and hydrogen peroxide-dependent signaling of stress responses in *Arabidopsis thaliana*. Proc Natl Acad Sci USA **104:** 672–677

Larsson O, Wennmalm K, Sandberg R (2006) Comparative microarray analysis. OMICS **10:** 381–397

Lee KP, Kim C, Landgraf F, Apel K (2007) EXECUTER1- and EXECUTER2-dependent transfer of stress-related signals from the plastid to the nucleus of *Arabidopsis thaliana*. Proc Natl Acad Sci USA **104:** 10270–10275

Levine A, Tenhaken R, Dixon R, Lamb C (1994) H_2O_2 from the oxidative burst orchestrates the plant hypersensitive disease resistance response. Cell **79:** 583–593

Li L, Li M, Yu L, Zhou Z, Liang X, Liu Z, Cai G, Gao L, Zhang X, Wang Y, et al (2014) The FLS2-associated kinase BIK1 directly phosphorylates the NADPH oxidase RbohD to control plant immunity. Cell Host Microbe **15:** 329–338

Li X, Zhang Y, Clarke JD, Li Y, Dong X (1999) Identification and cloning of a negative regulator of systemic acquired resistance, SNI1, through a screen for suppressors of *npr1-1*. Cell **98:** 329–339

Liszkay A, van der Zalm E, Schopfer P (2004) Production of reactive oxygen intermediates ($O_2 \cdot^-$, H_2O_2, and ·OH) by maize roots and their role in wall loosening and elongation growth. Plant Physiol **136:** 3114–3123, discussion 3001

Maeda H, Song W, Sage T, Dellapenna D (2014) Role of callose synthases in transfer cell wall development in tocopherol deficient *Arabidopsis* mutants. Front Plant Sci **5:** 46

Mandal MK, Chandra-Shekara AC, Jeong RD, Yu K, Zhu S, Chanda B, Navarre D, Kachroo A, Kachroo P (2012) Oleic acid-dependent modulation of NITRIC OXIDE ASSOCIATED1 protein levels regulates nitric oxide-mediated defense signaling in *Arabidopsis*. Plant Cell **24:** 1654–1674

Miller G, Mittler R (2006) Could heat shock transcription factors function as hydrogen peroxide sensors in plants? Ann Bot (Lond) **98:** 279–288

Mittal M, Siddiqui MR, Tran K, Reddy SP, Malik AB (2014) Reactive oxygen species in inflammation and tissue injury. Antioxid Redox Signal **20:** 1126–1167

Mittler R, Vanderauwera S, Gollery M, Van Breusegem F (2004) Reactive oxygen gene network of plants. Trends Plant Sci **9:** 490–498

Mittler R, Vanderauwera S, Suzuki N, Miller G, Tognetti VB, Vandepoele K, Gollery M, Shulaev V, Van Breusegem F (2011) ROS signaling: the new wave? Trends Plant Sci **16:** 300–309

Mor A, Koh E, Weiner L, Rosenwasser S, Sibony-Benyamini H, Fluhr R (2014) Singlet oxygen signatures are detected independent of light or chloroplasts in response to multiple stresses. Plant Physiol **165:** 249–261

Ng S, De Clercq I, Van Aken O, Law SR, Ivanova A, Willems P, Giraud E, Van Breusegem F, Whelan J (2014) Anterograde and retrograde regulation of nuclear genes encoding mitochondrial proteins during growth, development, and stress. Mol Plant **7:** 1075–1093

Oelze ML, Vogel MO, Alsharafa K, Kahmann U, Viehhauser A, Maurino VG, Dietz KJ (2012) Efficient acclimation of the chloroplast antioxidant defence of *Arabidopsis thalian* leaves in response to a 10- or 100-fold light increment and the possible involvement of retrograde signals. J Exp Bot **63:** 1297–1313

Oravecz A, Baumann A, Máté Z, Brzezinska A, Molinier J, Oakeley EJ, Ádám E, Schäfer E, Nagy F, Ulm R (2006) CONSTITUTIVELY PHOTOMORPHOGENIC1 is required for the UV-B response in *Arabidopsis*. Plant Cell **18:** 1975–1990

Page M, Sultana N, Paszkiewicz K, Florance H, Smirnoff N (2012) The influence of ascorbate on anthocyanin accumulation during high light acclimation in *Arabidopsis thaliana*: further evidence for redox control of anthocyanin synthesis. Plant Cell Environ **35:** 388–404

Paradis E, Claude J, Strimmer K (2004) APE: Analyses of Phylogenetics and Evolution in R language. Bioinformatics **20:** 289–290

Peng J, Li Z, Wen X, Li W, Shi H, Yang L, Zhu H, Guo H (2014) Salt-induced stabilization of EIN3/EIL1 confers salinity tolerance by deterring ROS accumulation in *Arabidopsis*. PLoS Genet **10:** e1004664

Pesaresi P, Hertle A, Pribil M, Kleine T, Wagner R, Strissel H, Ihnatowicz A, Bonardi V, Scharfenberg M, Schneider A, et al (2009) *Arabidopsis* STN7 kinase provides a link between short- and long-term photosynthetic acclimation. Plant Cell **21:** 2402–2423

Postnikova OA, Nemchinov LG (2012) Comparative analysis of microarray data in Arabidopsis transcriptome during compatible interactions with plant viruses. Virol J **9:** 101

Queval G, Neukermans J, Vanderauwera S, Van Breusegem F, Noctor G (2012) Day length is a key regulator of transcriptomic responses to both CO_2 and H_2O_2 in *Arabidopsis*. Plant Cell Environ **35:** 374–387

Redman JC, Haas BJ, Tanimoto G, Town CD (2004) Development and evaluation of an *Arabidopsis* whole genome Affymetrix probe array. Plant J **38:** 545–561

Rentel MC, Lecourieux D, Ouaked F, Usher SL, Petersen L, Okamoto H, Knight H, Peck SC, Grierson CS, Hirt H, et al (2004) OXI1 kinase is necessary for oxidative burst-mediated signalling in *Arabidopsis*. Nature **427:** 858–861

Rest JS, Wilkins O, Yuan W, Purugganan MD, Gurevitch J (2016) Meta-analysis and meta-regression of transcriptomic responses to water stress in Arabidopsis. Plant J **85:** 548–560

Rosenwasser S, Fluhr R, Joshi JR, Leviatan N, Sela N, Hetzroni A, Friedman H (2013) ROSMETER: a bioinformatic tool for the identification of transcriptomic imprints related to reactive oxygen species type and origin provides new insights into stress responses. Plant Physiol **163:** 1071–1083

Rosenwasser S, Rot I, Sollner E, Meyer AJ, Smith Y, Leviatan N, Fluhr R, Friedman H (2011) Organelles contribute differentially to reactive oxygen species-related events during extended darkness. Plant Physiol **156:** 185–201

Schwarzländer M, König AC, Sweetlove LJ, Finkemeier I (2012) The impact of impaired mitochondrial function on retrograde signalling: a meta-analysis of transcriptomic responses. J Exp Bot **63:** 1735–1750

Sewelam N, Jaspert N, Van Der Kelen K, Tognetti VB, Schmitz J, Frerigmann H, Stahl E, Zeier J, Van Breusegem F, Maurino VG (2014) Spatial H_2O_2 signaling specificity: H_2O_2 from chloroplasts and peroxisomes modulates the plant transcriptome differentially. Mol Plant **7:** 1191–1210

Shapiguzov A, Vainonen JP, Wrzaczek M, Kangasjärvi J (2012) ROS-talk: how the apoplast, the chloroplast, and the nucleus get the message through. Front Plant Sci **3:** 292

Smyth GK (2005) limma: Linear Models for Microarray Data. *In* R Gentleman, V Carey, W Huber, R Irizarry, S Dudoit, eds, Bioinformatics and Computational Biology Solutions Using R and Bioconductor. Springer, New York, pp 397–420

Stevens JR, Doerge RW (2005) Combining Affymetrix microarray results. BMC Bioinformatics **6:** 57

Suzuki N, Koussevitzky S, Mittler R, Miller G (2012) ROS and redox signalling in the response of plants to abiotic stress. Plant Cell Environ **35:** 259–270

Suzuki N, Miller G, Salazar C, Mondal HA, Shulaev E, Cortes DF, Shuman JL, Luo X, Shah J, Schlauch K, et al (2013) Temporal-spatial interaction between reactive oxygen species and abscisic acid regulates rapid systemic acclimation in plants. Plant Cell **25:** 3553–3569

Teng S, Keurentjes J, Bentsink L, Koornneef M, Smeekens S (2005) Sucrose-specific induction of anthocyanin biosynthesis in Arabidopsis requires the MYB75/PAP1 gene. Plant Physiol **139:** 1840–1852

Tognetti VB, Mühlenbock P, Van Breusegem F (2012) Stress homeostasis: the redox and auxin perspective. Plant Cell Environ **35:** 321–333

Tseng GC, Ghosh D, Feingold E (2012) Comprehensive literature review and statistical considerations for microarray meta-analysis. Nucleic Acids Res **40:** 3785–3799

Ulm R, Baumann A, Oravecz A, Máté Z, Ádám E, Oakeley EJ, Schäfer E, Nagy F (2004) Genome-wide analysis of gene expression reveals function of the bZIP transcription factor HY5 in the UV-B response of Arabidopsis. Proc Natl Acad Sci USA **101:** 1397–1402

Vaahtera L, Brosché M, Wrzaczek M, Kangasjärvi J (2014) Specificity in ROS signaling and transcript signatures. Antioxid Redox Signal **21:** 1422–1441

Van Breusegem F, Bailey-Serres J, Mittler R (2008) Unraveling the tapestry of networks involving reactive oxygen species in plants. Plant Physiol **147:** 978–984

Vanderauwera S, Zimmermann P, Rombauts S, Vandenabeele S, Langebartels C, Gruissem W, Inzé D, Van Breusegem F (2005) Genome-wide analysis of hydrogen peroxide-regulated gene expression in Arabidopsis reveals a high light-induced transcriptional cluster involved in anthocyanin biosynthesis. Plant Physiol **139:** 806–821

Viechtbauer W (2010) Conducting meta-analyses in R with the metafor package. J Stat Softw **36:** 1–48

Xu E, Vaahtera L, Brosché M (2015a) Roles of defense hormones in the regulation of ozone-induced changes in gene expression and cell death. Mol Plant **8:** 1776–1794

Xu E, Vaahtera L, Hõrak H, Hincha DK, Heyer AG, Brosché M (2015b) Quantitative trait loci mapping and transcriptome analysis reveal candidate genes regulating the response to ozone in *Arabidopsis thaliana*. Plant Cell Environ **38:** 1418–1433

Yi X, Du Z, Su Z (2013) PlantGSEA: a gene set enrichment analysis toolkit for plant community. Nucleic Acids Res **41:** 98–103

Supplemental Figure S1. Hierarchical clustering of transcriptional profiles and cluster identification. The relative extent of DEG overlap between all 157 transcriptional profiles was used to generate a dissimilarity matrix (1 - DSC, see Material and Methods) which was directly used for hierarchical clustering in R (average linkage). The resulting tree was cutted on a fixed threshold at a height of 0.8 (red dashed line). The resulting clusters consisting of at least 5 profiles
originating from minimum 2 studies were highlighted in red and blue.

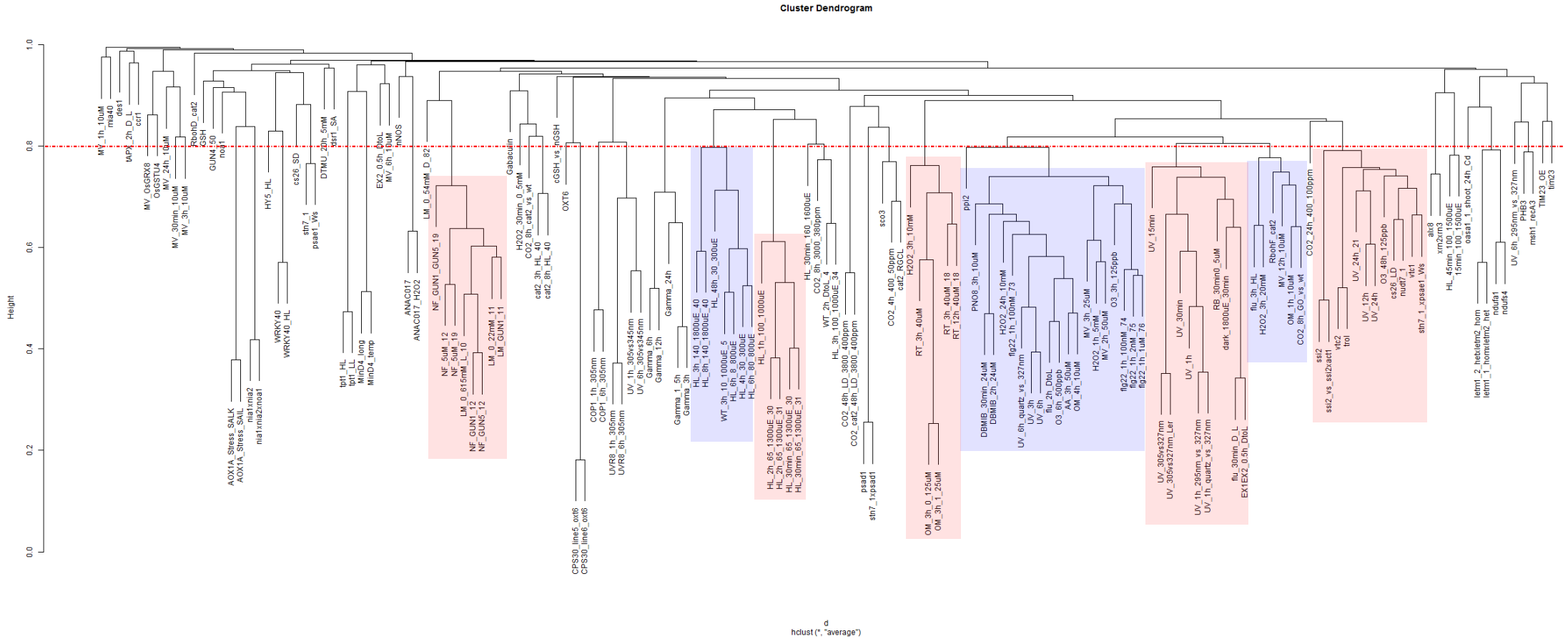

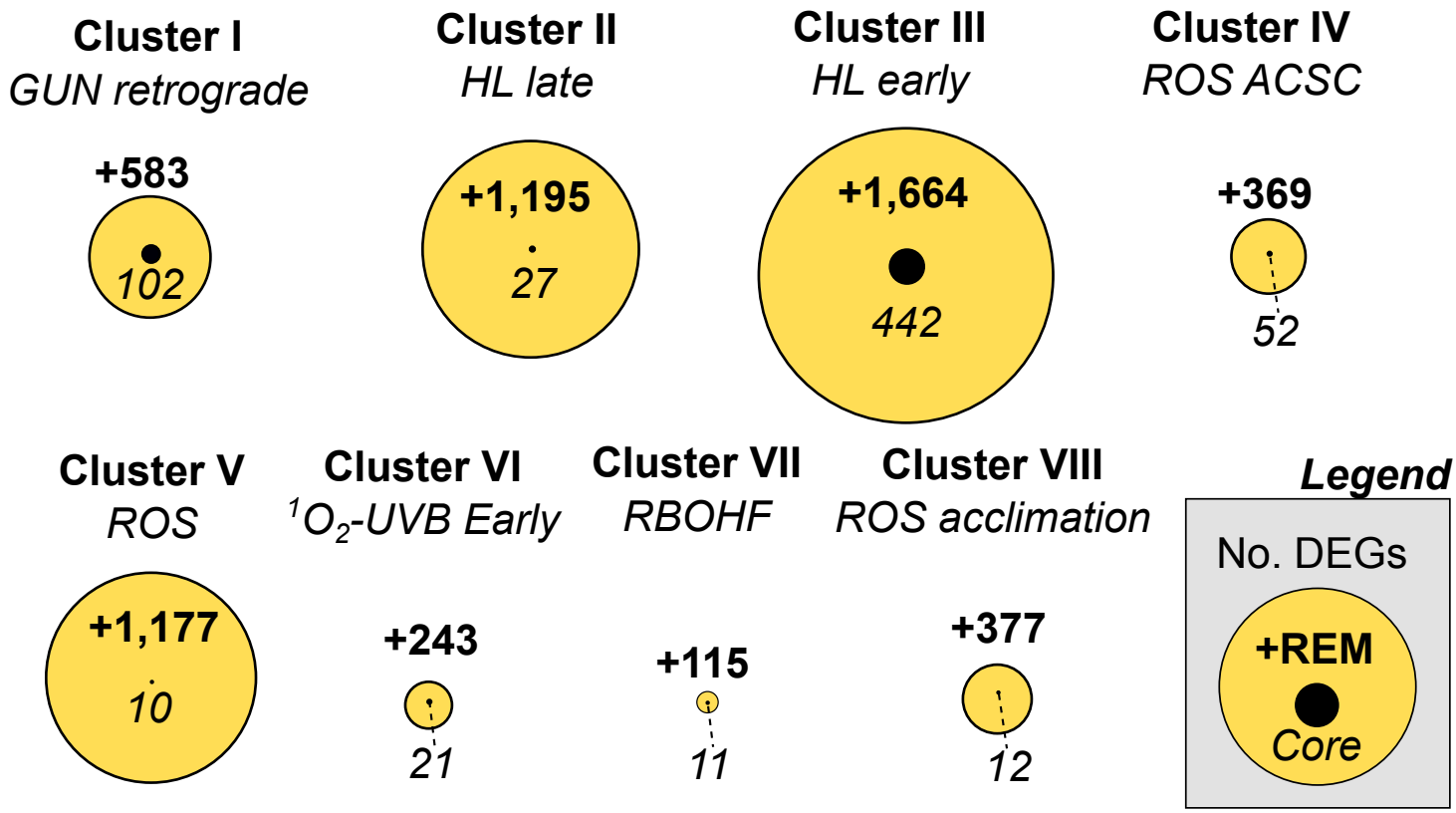

Supplemental Figure S2. Performance REM and traditional DEG list intersection approach. The amount of core DEGs, i.e. overlapping in all experiments, per cluster was represented as a black circle. All core DEGs were part of the DEGs identified by the REM procedure (yellow circle) and the additional (+) identified DEGs were indicated in bold. Circle size is scaled to the number of DEGs.

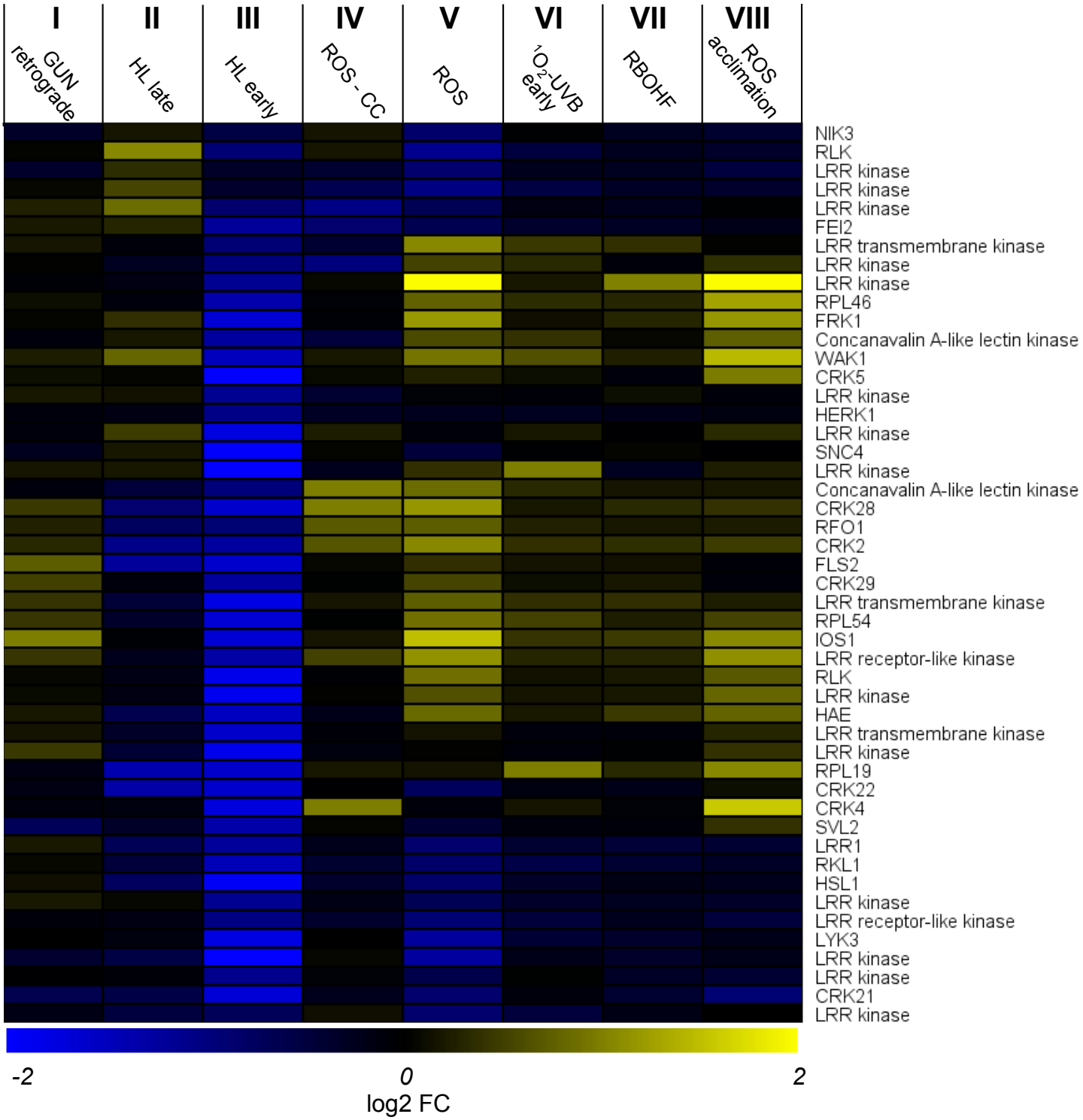

Supplemental Figure S3. Transcriptional regulation of receptor-like kinases (RLKs). Heatmap displaying the differential expression (log2 FC REM result) of RLKs which were differentially expressed in cluster III and/or IV. Abbreviations: CC, cell culture; CRK, cysteine-rich receptor-like kinase; GUN, GENOME UNCOUPLED; LRR, leucine-rich repeat; RbohF, respiratory burst oxidase homologueF.

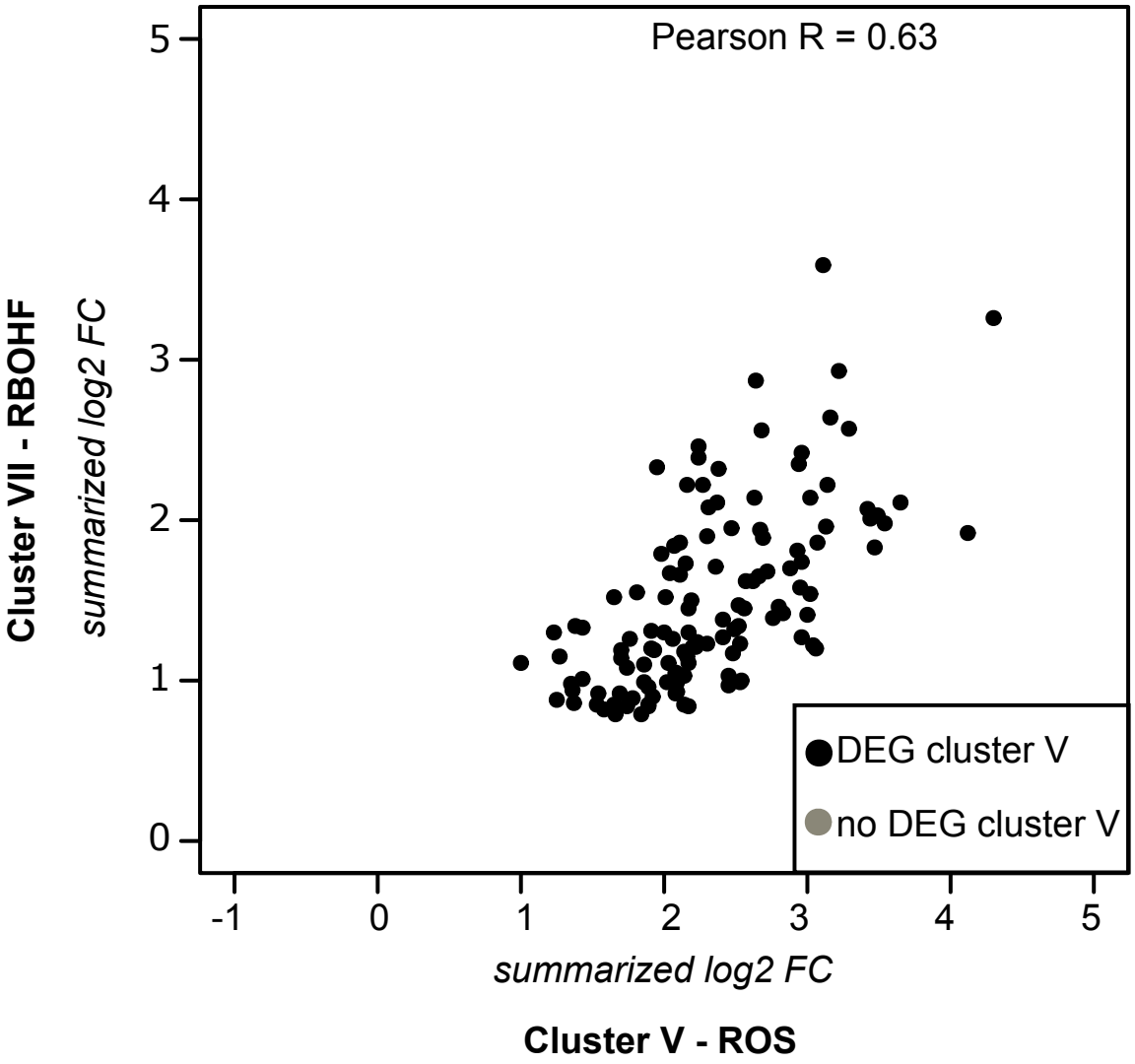

Supplemental Figure S4. Correlation and overlap of induced DEGs of RBOHF cluster VII with ROS cluster V. Summarized expression changes, as estimated by the REM, were plotted for cluster VII (y-axis) against those from cluster V (x-axis). Pearson correlation was specified and expression changes were colored black if differentially expressed in both clusters, or grey when only in cluster VII.

Supplemental Figure S5. Use of the cluster VIII footprint in the GENVESTIGATOR signature search tool (Hruz et al., 2008). The 355 significantly induced and 34 repressed genes of cluster VIII were used as signature to retrieve similar perturbations in Arabidopsis (all perturbations, euclidean distance).

Supplemental Figure S6. Use of the cluster VI footprint in the GENVESTIGATOR signature search tool (Hruz et al., 2008). The 264 significantly induced genes of cluster VI were used as signature to retrieve similar perturbations in Arabidopsis (all perturbations, euclidean distance).

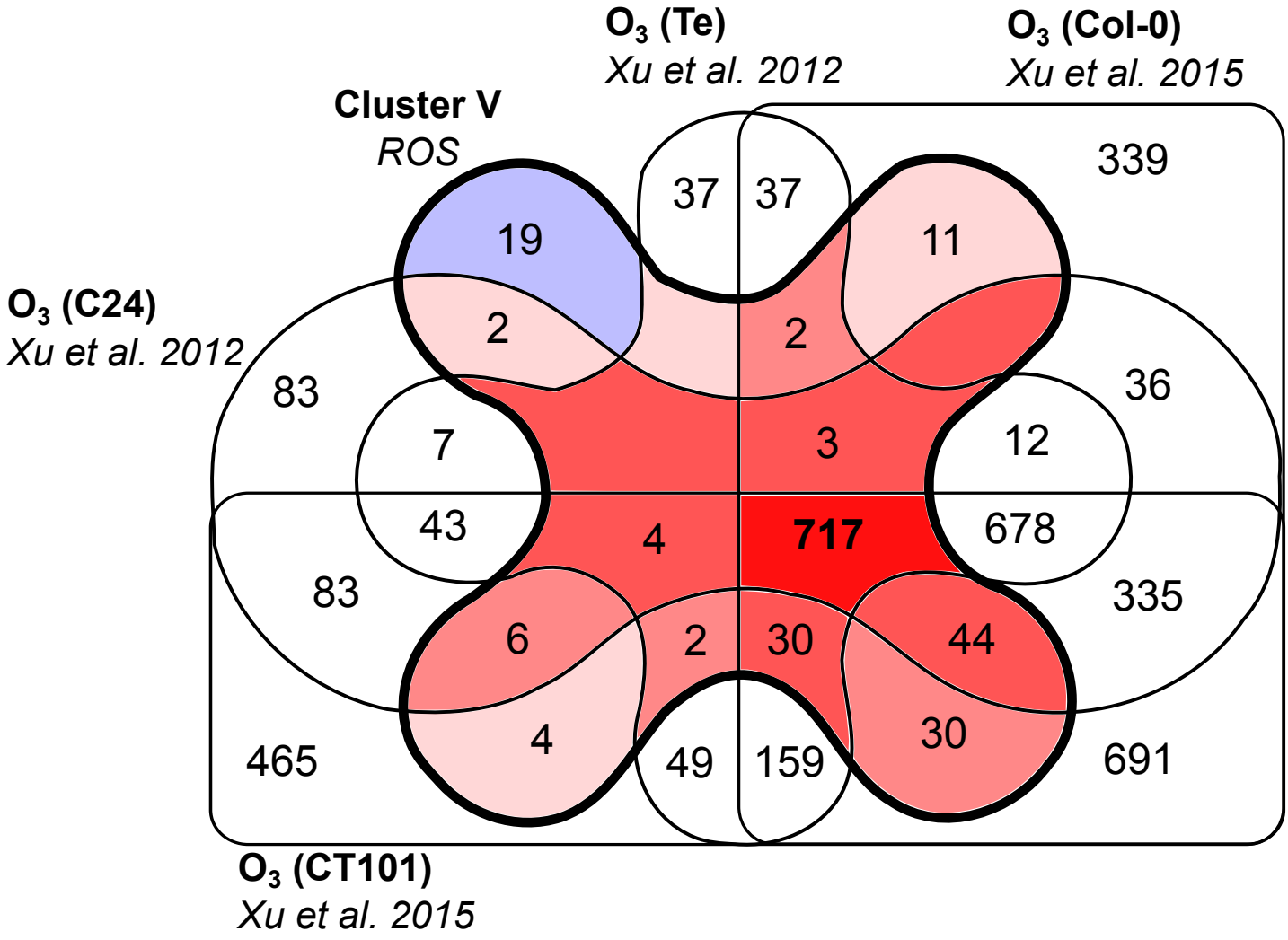

Supplemental Figure S7. Overlap of induced genes of ROS cluster V with ozone (O_3) RNA-Seq studies. The 874 induced genes (CI_{LB} > 0.58) of ROS cluster V were overlapped with ozone induced genes in Col-0 (Xu et al., 2015, Supplemental Table S5, adj. p-value < 0.05, log2 FC > 1) and three accessions (C24, Te, and CT101, Xu et al. 2012, FDR < 0.05, log2 FC > 1). The topology of ROS cluster V was outlined in bold. Non-overlapping DEGs of ROS cluster V were highlighted in blue, wheras highlighted more intense in red according the number of overlapping O_3 RNA-Seq studies.

SUPPLEMENTARY MATERIAL AND METHODS

Microarray data

Quality control

Microarray data quality was assessed by fitting a probe-level model using the 'affyPLM' package (version 1.38.0; Bolstad et al. 2005) of R/Bioconductor. Log2 intensity, normalized unscaled error rate and relative log expression plots were generated. GENEVESTIGATOR guidelines (http://genevestigator.com/userdocs/manual/qc.html) were followed in manual curation of all plots, i.e. alarming situations being respectively largely dissimilar box ranges in the probe intensity plot, boxes centered above 1.1 (normalized unscaled error rate plots) and dissimilar box ranges and/or not centered at 0 (relative log expression plots). In addition, the coherence of normalized expression values of replicate groups in each experiment was assessed by principal component analysis (PCA) and Pearson correlation plot. Here, clustering of replicated samples and separation with other replicate groups is sign of good quality. Depending on the quality assessment, certain microarray studies were not considered or some only partly by omitting profiled conditions containing microarray data of bad quality. After quality assessment, 680 CEL files of 79 independent studies were retained (Supplemental Table S1).

In-house microarray data

In total four ATH1 unpublished microarrays experiments were included in our meta-analysis. Experimental details are provided below for the microarray experiments. All extracted RNA was hybridized to ATH1 arrays at the VIB Nucleomics Core (http://nucleomics.be) according to manufacturer's instructions.

A) 10mM H_2O_2 treatment

Seeds were surface-sterilized by fumigation overnight and cold treated at 4ºC for 3-4 days before germination in 96-well plates (5 seeds/well) containing half-strength liquid Murashige and Skoog (MS) medium supplemented with 1% sucrose (0.2 ml/well). Plants were grown under controlled environmental conditions (16 h/8 h light/dark, 100 $\mu mol \cdot m^{-2} \cdot s^{-1}$ light intensity, 21ºC, 70% relative humidity). After 9 days, H_2O_2 was added to a final concentration of 10 mM. Control plants were treated with the same volume of water. Seedlings were harvested after 24 h and total RNA was isolated using Trizol Reagent (Life Technologies, Gaithersburg, USA).

B) 400 to 100 ppm CO_2 shift

Plants were grown in soil under normal (400 ppm) CO_2 conditions. After 6 weeks plants were transferred to low CO_2 conditions (100 ppm) during 24 h or kept at 400 ppm CO_2 (control condition). For each replicate plant leaf material was pooled from 4-5 individual plants and total RNA was isolated using Trizol Reagent (Life Technologies, Gaithersburg, USA).

C) 24h Restricted Gas Continuous Light Conditions

Wild-type and *cat2-2* seeds were surface-sterilized by fumigation overnight and cold treated at 4ºC for 2 days before germination and grown on full-strength MS medium with vitamins supplemented with 1% sucrose for 3 weeks under controlled conditions at 21°C under short day 8 h light (100 $\mu mol \cdot m^{-2} \cdot s^{-1}$)/16 h dark regime. After 21 days plants were subjected Restricted Gas Continuous light conditions during 24 h by replacing the surgical tape that sealed the plates (Micropore, City Country, USA) by two layers of parafilm M (Bemis, Oshkosh, USA) to restrict gas exchange between the plate and the outside environment and by transferring to a continuous light regime (100 $\mu mol \cdot m^{-2} \cdot s^{-1}$). Shoot tissue from both genotypes was sampled in three biological replicates before and after 24 h of treatment. Each replicate consisted of at least 15 rosettes. RNA was extracted with Spectrum Plant Total RNA Kit (Sigma, St. Louis, USA).

D) *cat2 rbohD and cat2 rbohF* photorespiratory stress

Plants were grown in air from seeds under a 16 h/8 h day/night regime, relative humidity was 65%, and an irradiance of 200 $\mu mol \cdot m^{-2} \cdot s^{-1}$ was used to drive oxidative stress in the *cat2* background plants. Arabidopsis Col-0, *cat2*, *cat2 rbohD* and *cat2 rbohF* were 3 week old before sampling. Three biological replicates were generated each consisting of a pool of leaves from at least 8 plants.

RNA Sequencing

Cat2-2 mutant plants were grown under elevated CO_2 concentrations (3,000 ppm) to impair photorespiration. Individual plants were organized according to a completely randomized block design in a controlled climate chamber (Vötsch Industrietechnik, Balingen, Germany) in a 16 h/8 h day/night regime (relative humidity of 75%, 21°C and an irradiance of 120 $\mu mol \cdot m^{-2} \cdot s^{-1}$). For high light treatments, 3-week-old plants were transferred to a Sanyo Fitotron (Weiss Technik, Leicestershire, UK) plant growth chamber in ambient air conditions (400 ppm CO_2, relative

humidity of 55%, 21°C) and irradiation of 1,200 $\mu mol \cdot m^{-2} \cdot s^{-1}$ for three hours. Middle aged leaves of 15 individual plants per line were sampled, pooled and frozen in liquid nitrogen. This entire set-up was repeated to obtain three biological repeats. RNA was extracted using a combination of TRIzol and RNeasy Kit (Qiagen) according to the manufacturers' instructions.

Library preparation and sequencing was performed at the VIB Nucleomics Core (www.nucleomics.be). Sequencing libraries were constructed using the TruSeq Stranded mRNA Library Preparation Kit (Illumina). Three biological replicates were sequenced on Illumina NextSeq 500, resulting in approximately 30 million 75 bp single end reads per sample. Raw sequence files can be consulted under the GEO accession code GSE77171. Adapter sequences and low quality base-pairs ($Q < 20$) were trimmed using Trim Galore (v0.3.3, http://www.bioinformatics.babraham.ac.uk/projects/trim_galore/), retaining high-quality reads of at least 40 bp length. Quality-filtered reads were aligned to the TAIR10 Arabidopsis reference genome using the spliced aligner TopHat2 (v2.1.0, Kim et al. 2013). The number of reads per gene was quantified using the featureCounts function as implemented in the Subread package (v1.4.6, Liao et al. 2014). Only reads mapping to protein coding genes (as annotated in TAIR10) were retained. Differentially expressed genes (DEGs) were identified using the R (v3.1.2) software package edgeR (Robinson et al. 2010). For further analysis, only genes with expression values higher than 0.21 cpm (corresponding to 5 read counts) in at least 3 samples were retained (19,012 genes). TMM normalization (Robinson and Oshlack 2010) was applied using the calcNormFactors function. Variability in the dataset was assessed with a MDSplot to calculate pairwise distances. There was a clear separation according photorespiratory stress. To test user-defined hypotheses, a no-intercept single factor model was defined according to stress treatment (*cat2* 3 h versus 0 h stress). Dispersions were estimated using the estimateGLMRobustDisp function. A negative binomial regression model was then used to model the overdispersed counts for each gene separately with fixed values for the dispersion parameter as outlined in McCarthy et al. 2012) and as implemented in the function glmFit using the above described model. Hypothesis testing was based on likelihood ratio tests. False discovery rate adjustments of the p values were performed with the method described by Benjamini and Hochberg 1995).

REFERENCES

Benjamini, Y. and Y. Hochberg (1995). "Controlling the False Discovery Rate - a Practical and Powerful Approach to Multiple Testing." Journal of the Royal Statistical Society Series B-Methodological 57(1): 289-300.

Bolstad, B. M. C., F.; Brettschneider, J.; Simpson, K.; Cope L.; Irizarry, R.A.; and Speed, T.P. (2005). Quality Assessment of Affymetrix GeneChip Data. Bioinformatics and Computational Biology Solutions using R and Bioconductor. R. C. Gentleman, V.; Huber, W.; Irizarry, R.A.; and Dudoit, S. . New York, Springer: 33-47.

Kim, D., G. Pertea, C. Trapnell, H. Pimentel, R. Kelley and S. L. Salzberg (2013). "TopHat2: accurate alignment of transcriptomes in the presence of insertions, deletions and gene fusions." Genome Biol 14(4): R36.

Liao, Y., G. K. Smyth and W. Shi (2014). "featureCounts: an efficient general purpose program for assigning sequence reads to genomic features." Bioinformatics 30(7): 923-930.

McCarthy, D. J., Y. S. Chen and G. K. Smyth (2012). "Differential expression analysis of multifactor RNA-Seq experiments with respect to biological variation." Nucleic Acids Research 40(10): 4288-4297.

Robinson, M. D., D. J. McCarthy and G. K. Smyth (2010). "edgeR: a Bioconductor package for differential expression analysis of digital gene expression data." Bioinformatics 26(1): 139-140.

Robinson, M. D. and A. Oshlack (2010). "A scaling normalization method for differential expression analysis of RNA-seq data." Genome Biol 11(3): R25.